Check for updates

Materiomics approaches for stimuli-responsive microrobots

Silvia Orecchio,[a] Giuseppe Arrabito, (ID) *[a] Claudia Pellerito,[a] Tiziana Fiore, (ID) [a] Floriana Campanile,[b] Federica Meringolo,[c] Paola Costanzo, (ID) [c] Sebastiano Alberto Fortuna,[b] Salvatore Barreca,[d] Giorgia Puleo,[a] Vittorio Ferrara[a] and Bruno Pignataro (ID) *[a]

The development of stimuli-responsive smart materials able to perform "on-demand" tasks is one of the most enticing interdisciplinary challenges in science. In the last decade, synthetic micro/nanorobots have shown enormous potential in this regard by overcoming the time reversal motion symmetry at low Reynolds numbers, so conferring dissipative motion for the active exploration of complex fluids in the field of sensing, capturing and targeting analytes in desired locations. This review presents a critical overview of inorganic/organic materials and their combination aiming for sustainable microrobot fabrication through a materiomics approach, ultimately highlighting their structure–function correlation for future applications related to the removal of environmental pollutants. A rational selection of materials combination by leveraging sustainable fabrication approaches will be presented, ultimately classifying the resulting microrobots as a function of their efficiency in terms of bespoke quantitative parameters (microrobot materials, size, speed, stability, and reconfigurability) and finally introducing the field of biohybrid microrobots.

1. Introduction

The design of novel materials for environmental remediation is a growing research field, driven by the demanding need to address the pollution resulting from industrial and human waste, as recently reviewed in the EU's Urban Wastewater Treatment Directive.[1] Indeed, new pollutants, such as dyes, pharmaceuticals, organic contaminants, microplastics, metal ions and per-/polyfluoroalkyl substances, require the design of technologies that are suitable for their monitoring[2] and treatment.[3] Importantly, such a challenge requires the adoption of new treatment technologies, advancing the established methods.[4]

In this scenario, use of micro- and nanoscale robots, defined as microscopic systems featuring autonomous actuation capability, ranging in size from 1 μm to 1 mm[5] is being currently explored as a suitable strategy.[6] In general terms, robots can be defined as machines programmed to perform specific tasks autonomously or under human supervision. More specifically,

the research activities on robotics have focused on two opposite directions, namely giant and micro-/nano-scale systems, both capable of autonomously performing complex tasks once programmed.[7] As the name suggests, "microrobots" refer to any type of robot of submillimeter size. Small-scale robots (<100 μm), initially referred to as 'micro- and nanomotors', are micro- and nanostructured materials capable of harvesting energy from the surrounding environment and converting it into locomotion. In general, a microrobot can be defined as a device of micrometer to millimeter size that can move, apply forces and operate on objects in a workspace of micrometer or submicrometer dimensions.[8] Such devices benefit from the synergy between their motion attributes and their unique size-, shape- and structure-dependent physicochemical properties at the micro- and nanoscales. Furthermore, they show superior performance compared to passive matter (for example, conventional static micro- and nanomaterials) in all areas, including water remediation.[9] In turn, nanorobots can be defined as molecular or nanoscale devices that convert different external energy sources into self-propelling motion[10] and as systems that are able to perform specific tasks at the atomic or molecular level.[11]

The advantage of smaller sized robots in comparison to macroscale robots lies in their ability to swim in liquid environments, which are difficult to explore for humans (*i.e.* small sizes or hazardous sites). In particular, microswimmers are a subdivision of microrobots with the ability to move in liquids

[a] *Department of Physics and Chemistry – Emilio Segrè, University of Palermo, Building 17, Viale delle Scienze Palermo 90128, Italy.*
   E-mail: giuseppedomenico.arrabito@unipa.it, bruno.pignataro@unipa.it
[b] *Department of Biomedical and Biotechnological Sciences (BIOMETEC), University of Catania, 95123, Catania, Italy*
[c] *Department of Chemistry and Chemical Technologies, University of Calabria, 87036, Rende, Italy*
[d] *Department of Chemical Sciences, University of Catania, Viale Andrea Doria, 6, 95125, Catania, Italy*

19576 | *J. Mater. Chem. C*, 2025, **13**, 19576–19600

This journal is © The Royal Society of Chemistry 2025

(*e.g.*, bodily fluids or water) autonomously or under external actuation. Nonetheless, the term "microswimmers" has been in use for natural micron-sized swimmers (*e.g.*, bacteria, sperms, archaea, and protists), even before the invention of microrobots. Therefore, neither "microrobots" nor "micro-swimmers" can be considered a full subset of the other one – not all microrobots are microswimmers and *vice versa*.[12]

While the function of macro-robots is controlled by inertial forces, micro- and nanorobot (MNM) actuation is based on a substantially different theoretical framework. In 1976, Pursell's "scallop theory" demonstrated that the time-symmetric movement of an object in miniaturized systems and hence low Reynolds number scenarios do not lead to net displacement.[5] As a consequence, the condition proved by this theorem needs to be violated to displace micro/nanorobots.

MNMs can be fabricated by employing scalable approaches based on different strategies, such as physical vapor deposition, electrochemistry or rolling technology.[13–15] Similarly to macro-scale robots that typically have sensors and actuators, a control unit and an external energy input,[13] MNMs convert external triggers (magnetic fields, ultrasound, chemical fuels, and light) into net displacement for specific applications.[16] As a result, such controllable stimuli, micro- and nano-robots are able to absorb and destroy specific pollutants in the absence of convective motions. In addition, enzyme immobilization can further improve motion ability or enzymes can act as components to catalyze decontamination reactions.[17,18] A recent review on this topic has explored the range of pollutants these microrobots can target.[6]

A significant challenge is to develop fully functional microrobots capable of autonomously operating in complex environments. Imitating nature is a suitable strategy to install sensing, actuation and control directly through the materials. Nature, in fact, provides many examples of nanomotors in living cells. A compelling question is whether it is possible to realize artificial nano- to micro-robots competing with nature biomotors. Cells use nano-engines to change shape, separate chromosomes during division, synthesize proteins, engulf nutrients, and transport chemicals. Basically, all these motors convert chemical energy, usually stored as adenosine triphosphate, into active motion.[19] As reported in Table 1, the propulsion mechanism of MNMs can be exploited by different means, such as magnetic, optical, chemical or hybrid, enabling different means to control the movement of such systems.

Questions that are then obvious for the materials scientists are how are these micro- and nanorobots prepared, which are the most common formulations used in the previous reports and finally the discovery of optimal formulations based on structure–function relationships. To this end, a study was conducted through extensive search of the terms micromotors, microrobots and microswimmers in two electronic databases: Scopus and Web of Science. The search identified a total of 1177 articles, of which 446 came from Scopus and 731 from the Web of Science. These articles deal with the development of MNMs, with particular attention to the materials used for their

Silvia Orecchio received her Master's Degree in Chemistry and Pharmaceutical Technologies (2019) and her PhD in Molecular and Biomolecular Sciences (2024) from the University of Palermo, with activities also carried out at IMDEA Nanociencia (Madrid) and Eni S.p.A. (Novara). She worked on molecular and polymeric materials for perovskite photovoltaic devices, contributing to their characterization, assembly and testing. Previously, at the University of Pavia, she conducted gas chromatographic studies on substances obtained from combusted sites. She is currently a research fellow in Palermo, where she studies the potential release of contaminants from photovoltaic and optoelectronic devices.

Silvia Orecchio

Giuseppe Arrabito received his BSc in Chemistry and MSc in Bio-molecular Chemistry at the Scuola Superiore di Catania. After a PhD (2012) in Nanoscience from Scuola Superiore di Catania, he was a Post-Doctoral fellow at the Technical University of Dortmund and at the University of Rome Tor Vergata. Since 2024, he is Associate Professor of Analytical Chemistry at the University of Palermo. His research lies at the interface of synthetic biology, DNA nano-technology, and zinc oxide-based devices.

Giuseppe Arrabito

Bruno Pignataro obtained his PhD degree in Materials Science from the University of Catania. He is a Full Professor of Physical Chemistry at the University of Palermo. He is a referee and editorial board member for many journals and an expert evaluator for national and international research proposals. He is the Project Leader of the District of High Technology for innovation in the field of Cultural Heritage in Sicily. His research interests are in the topics of nanotechnology, molecular surfaces, plastic electronics, and biotechnology.

Bruno Pignataro

This journal is © The Royal Society of Chemistry 2025

J. Mater. Chem. C, 2025, **13**, 19576–19600 | **19577**

Table 1 Strengths and weaknesses of the means of locomotion of MNRs

Propulsion stimulus	Strengths	Weaknesses	Bibliographic references
Magnetic field	Established fabrication technologies, biocompatibility	Difficulty retrieving the device in complex environments	Bozuyuk et al.,[20] 2018 Yang et al.,[21] 2025 Senthilnathan et al.,[22] 2025 Maria-Hormigos et al.,[23] 2025
Light	Easy control and accessible optical energy	Motility impacted by the surrounding environment	Zhou et al.,[24] 2017 Geng et al.,[25] 2024 Ikram et al.,[26] 2024 Yuan et al.,[27] 2025
Chemical fuels	Simple design, numerous types of reactions to adapt in different environments	Use of potentially toxic fuels	Magdanz et al.,[28] 2014 Panda et al.,[29] 2018 Peng et al.,[30] 2019 Liu et al.,[31] 2024 Xiao et al.,[32] 2025
Hybrid (biological entity + external stimulus)	Biocompatibility and adaptation to various energy sources	Complex design	Li et al.,[33] 2015 Peng et al.,[34] 2024 Li et al.,[35] 2025 Wang et al.,[36] 2025

fabrication. Scientific data published from 2014 to date were considered. The search strategy was carefully developed, using specific search terms and Boolean operators. The aim was to identify scientific articles on different materials employed in the fabrication of micro-and nanorobots, with various mechanisms and intended for multiple applications, from environmental decontamination to medical uses. The selected keywords allowed us to exclude irrelevant articles and focus on relevant publications. The search covered articles published from 2014 to 2024, resulting in a comprehensive overview of the current state of the field.

MNMs are distinguished not only by their size and applications, but also by the materials they are made of. For this reason, the focus has been directed towards the various materials most studied in the last decade, since the choice of materials not only influences the operational capabilities of robots, but also determines their compatibility with biological and industrial environments. Most of the articles are concerning the use of titanium as the prevalent material, either as titanium oxide or in combination with other materials, with a total of 213 articles found on Scopus and 199 on the Web of science (see Fig. 1). Other materials widely used in robots' fabrication include carbon and its allotropes, particularly graphene, whose use has been widely documented in the literature. Specifically, 148 and 215 articles were found respectively on Scopus and the Web of Science, by entering only the words "carbon" and "micromotor/robot and nanorobot". This search is understandably narrowed for "graphene-based robots" to a smaller number of articles due to their more specialized nature.

In this context, the concept of materiomics becomes particularly relevant, as it refers to the study of how the physicochemical properties of materials influence their function in complex systems. In general, the term materiomics refers to a comprehensive approach that studies materials in a holistic way by analyzing their properties and interactions across different scales to better understand and optimize their performance in microrobots.[37,38] In particular, when applied to micro- and nanorobots, this perspective focuses on how structural and
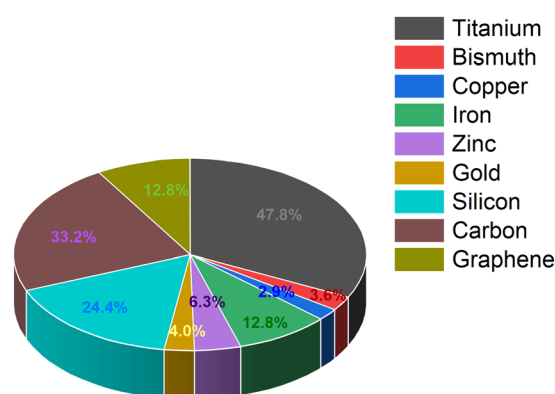
Fig. 1 Materials used in the manufacture of microrobots. Percentage distribution of materials or elements used for the fabrication of micro/nano-motors and robots, with graphene, carbon and silicon being among the main components, at 33.2%, 24.4% and 47.8%, respectively. Data extracted from the Scopus database.

compositional characteristics such as morphology, surface chemistry, crystalline phases and responsiveness to external stimuli affect performance in terms of motion, interaction with the environment and degradation of pollutants.

This review adopts a materials-centred perspective to analyse recurring patterns and correlations between material types and the functional capabilities of these systems, with the aim of highlighting how specific material choices condition the actuation mechanisms and application potential of micro- and nanorobots, particularly in the context of environmental remediation. For this reason, the focus has been directed towards the various materials most studied in the last decade. Differently from other reviews in the field, which focus on materials consideration analysis for microrobots for various applications,[39,40] herein we intend to provide the reader with a systematic discussion focusing on materiomics approaches for microrobot fabrication, targeting applications in the field of pollutant degradation, as a promising and still poorly explored aspect of this groundbreaking technology.

Among these microrobots, significant attention has been given to the development of titanium dioxide-based microrobots. However, due to their limited absorption, over the years, alternative microrobots using semiconductors that absorb light in the visible and near-infrared region have also been explored. The substantial progress in this field has led to the development of high efficiency light-driven microrobots, leveraging visible-light-sensitive photocatalysts, including Fe_2O_3, CdS, and Ag_3PO_4. To improve the separation of the electron–hole pair, Janus particles with metal–semiconductor heterostructures, such as C_3N_4/Pt, Cu_2O/Au, and BiOI/Au, have been used. Photocatalysts such as $BiVO_4$ with bandgaps in the visible range lead to the development of photocatalytic microrobots with improved movement speed and capacity. Finally, new emerging approaches based on innovative materials and biohybrid microrobots are presented. Ultimately, materiomics could allow developing novel materials having desirable functionalities for pollutant degradation by examining how different components interact and behave at various levels of organization.

2. Titania based microrobots

Among the different materials used to fabricate microrobots, TiO_2 allotropes have shown outstanding success in photocatalysis[41,42] based processes, owing to their nontoxicity, ease of synthesis and potential for bandgap engineering.[43]

The motion of micro- and nanorobots (MNMs) occurs in fluids with low Reynolds numbers, where viscous drag prevails over inertial forces; therefore, their mobility requires a constant application of propulsive force. Illumination triggers redox reactions that develop solute gradients. The net directional motion of MNMs is based on an asymmetric propulsive force, which is achieved through structural asymmetry or light gradient asymmetry, *via* autoelectrophoresis and self-diffusionphoresis. However, as a result of rapid electron–hole pair recombination, photocatalytic reactions tend to have low efficiency. To increase the yield, these pairs can be more efficiently separated through doping, metal loading or formation of heterojunctions.[44]

The use of hybrid materials, characterized by intrinsic structural asymmetry, offers several advantages such as the reduction of the required light intensity and fuel concentration (*e.g.* H_2O_2, N_2H_4, and Br_2) and expanded applications of MNMs. To find viable alternatives to fuel-free MNMs, MNMs based on TiO_2/metal heterojunctions have been developed in which metal components allow for better separation of electron–hole pairs, thus avoiding recombination. At heterojunctions, electrons migrate to the metal surface, while holes move toward TiO_2 creating redox splits. This process generates a proton gradient from the TiO_2 surface toward the metal surface, driving motion.[45]

Photocatalytic microrobots have proven to be excellent candidates for pollutant degradation by exploiting the synergy between self-propulsion and the photocatalytic effect.[46] The latter can be selectively activated based on irradiation type, while self-propulsion is linked to hydrogen peroxide decomposition that occurs through asymmetric illumination of the particles. Microrobots that exploit TiO_2 have been studied, such as core–shell TiO_2/carbon microsphere microrobots, where TiO_2 serves to photocatalyze chemical reactions and the degradation of unwanted organic substances.
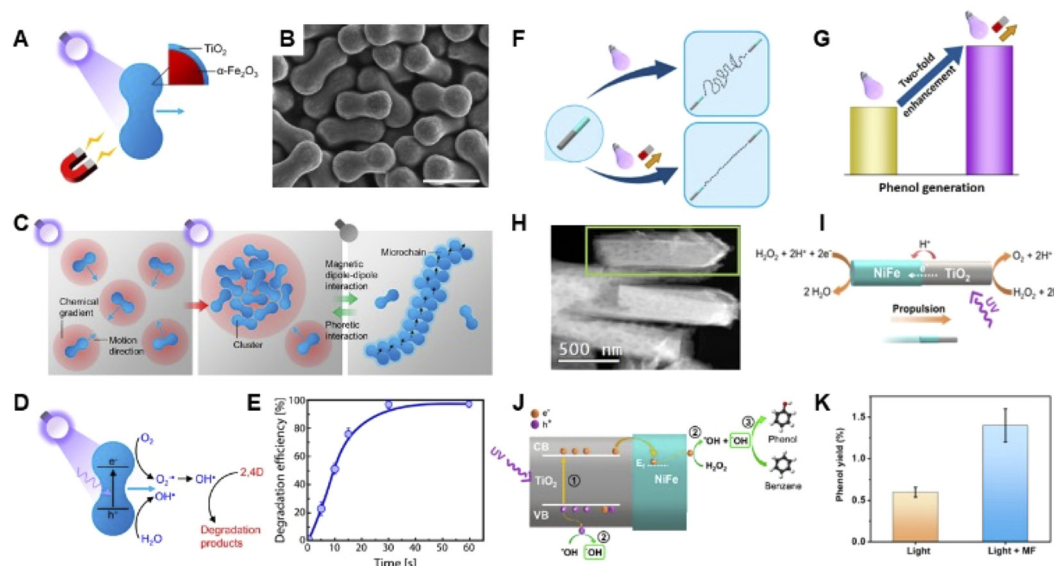
Using two photocatalytic semiconductors, a hybrid microswimmer has been developed, capable of decomposing peroxide at different speeds depending on the color of the activation light source. These particles therefore move depending on the irradiation wavelength. Hybrid microrobots based on titanium dioxide (TiO_2) and cuprous oxide (Cu_2O) have been produced,[47] with the materials occupying distinct portions of the particles. The study has shown that hybrid structures' movement depends on the wavelength, unlike those made from just one of the two materials, Moreover, hybrid particles activate solely in water, enabling the development of new classes of photosensitive colloids that do not require fuel.

Chemical reactions catalyzed on the surface of a particle have been exploited to obtain movements on a microscopic scale. In these systems, the position of the catalyst (reactive structure) and the shape of the particle are fundamental for the movement. Combining multiple catalysts into a single particle can therefore enable modifications to the system's motion.

The fabrication of heterostructures composed of different types of semiconductors represents a valid alternative. In this context, the use of α-Fe_2O_3 has been developed thanks to its advantageous properties, such as photoactivity, biocompatibility, and more. Microrobots have been designed to utilize light radiation for movement and pollutant degradation, and magnetic fields for their subsequent collection,[48] see Fig. 2(A)–(C). Under light or magnetic fields triggers, microrobots can self-assemble into porous structures or aggregates, enabling them to trap and photodegrade pollutants. They can also reconfigure into linear shapes and, with the aid of magnetic fields, remove debris such as micro- and nanoplastics from water. Their ability to select and detect specific particles provides a visual indication of pollutant distribution. Furthermore, their magnetic properties allow for the easy recovery of microrobots from purified water. The reversibility of their self-assembly has been demonstrated by turning UV light on and off. Additionally, leveraging their photocatalytic activity and self-propulsion capability, microrobots have proven effective in accelerating photocatalysis, such as in the degradation of the herbicide 2,4-dichlorophenoxyacetic acid (2,4-D) as reported in Fig. 2(D) and (E). Considering the widespread use of pesticides in agriculture and the associated contamination and pollution risks, self-propelled microrobots composed of TiO_2/α-Fe_2O_3 have been used to accelerate the photocatalytic degradation of this persistent and carcinogenic herbicide. The microrobots achieved a degradation efficiency of 97% within 30 minutes under light exposure. The degradation mechanism is linked to the interaction between the photocatalyst irradiation and water, leading to the formation of reactive oxygen species capable of breaking the chemical bonds of the undesirable substance. Unlike other systems these microrobots offer the advantage of not requiring H_2O_2. Differently to established photocatalysts, TiO_2/α-Fe_2O_3 microrobots were able to destroy degraded the same amount

This journal is © The Royal Society of Chemistry 2025

J. Mater. Chem. C, 2025, **13**, 19576–19600 | **19579**

Fig. 2 Design, structure, and photocatalytic performance of TiO$_2$/α-Fe$_2$O$_3$ microrobots and TiO$_2$/NiFe nanomotors. (A) Schematic illustration of TiO$_2$/α-Fe$_2$O$_3$ microrobots with light- and magnetically driven motion. (B) SEM image of peanut-shaped α-Fe$_2$O$_3$ particles, scale bar 2 μm. (C) Self-assembly behaviour under chemical gradients and magnetic dipole−dipole interactions forming clusters and microchains. (D) Photocatalytic mechanism of dichlorophenoxyacetic acid (2,4-D) degradation via ROS generation mediated by UV light. (E) Graph showing time-dependent degradation efficiency of 2,4-D, reaching 97% in 30 minutes. Adapted with permission from Nature Communications, ref. 48 Copyright©2023. This is an open access article distributed under the terms of the Creative Commons CC BY license. (F) Schematic illustrating the motion behaviour of TiO$_2$/NiFe nanomotors under UV light and magnetic fields. (G) Representation of improved photocatalytic phenol generation by the combined effects of light and magnetic fields. (H) STEM image of TiO$_2$/NiFe nanomotors. (I) Photocatalytic propulsion mechanism of TiO$_2$/NiFe nanomotors mediated by UV light, driven by electron transfer and H$_2$O$_2$ decomposition. (J) UV light-induced electron excitation in TiO$_2$ and charge transfer to NiFe, generating ROS that oxidize benzene to phenol. (K) Phenol yield comparison under light and light + magnetic field conditions, showing enhanced performance. Reprinted with permission from ACS Applied Materials & Interfaces, ref. 50 (ACS) Copyright©2023. (**https://pubs.acs.org/doi/10.1021/acsami.4c03905**). Readers are advised that any requests for additional permissions relating to the extracted material must be addressed directly to ACS.

of 2,4D in less time, since their movement result in more collisions with the pollutant molecules per unit of time. It has been highlighted that microrobots exploit the decomposition of water into oxygen and oxide radicals for movement. Thanks to this mechanism they have been designed for use in photocatalysis and for drug delivery. In recent years, a study has shown that CoO microparticles demonstrate photocatalytic activity when irradiated with visible light, unlike TiO$_2$ which requires UV light, resulting in a CoO–TiO$_2$ heterojunction, which exploits both the UV and visible light for their action.[49] This type of microrobot can also be oriented by varying the wavelength of the incident radiation, without relying on phototaxis.

A significant percentage of artificial microrobots generate propulsion by utilizing the interaction between asymmetric gradients and the surface of the particles. The ideal mechanism to break symmetry is the Janus geometry, where the differing chemical reactivity of the two halves promotes the generation of an asymmetric gradient. It has been demonstrated that producing TiO$_2$ particles with a rutile conformation structured in a Pac-Man shape through a one-pot synthesis process results in active motion only for particles that underwent calcination processes.[51] Specifically, only the particles with asymmetric structures after calcination demonstrated crystallinity sufficient to meet both requirements for active matter.

Photocatalytic nanomotors have garnered great interest since they can convert light radiation and chemical energy into motion at the same time, coupled with a rapid photoelectric response. It has been demonstrated that combining optical and magnetic components within these nanodevices not only enables precise control over their motion, but also enhances their photocatalytic activity with higher efficiencies.[50] In this regard, a notable example is the development of heterojunction TiO$_2$/NiFe nanomotors, composed of TiO$_2$ nanorods coupled with the Ni/Fe metallic counterpart. These nanomotors exhibit excellent photoactivity under UV light, achieving self-propulsion with random trajectories. When combined with the magnetic field, their alignment results in more directional motion and enhanced speeds, showcasing their advanced functionality as microrobots, as can be seen in Fig. 2(F)–(K).

Over the years, various metal-based sensors have been developed for gas and analytes in solution detection.[52,53] TiO$_2$ has proven to be an excellent candidate in this field due to its good electron mobility, suitable band gap, and high stability. However, to address the growing need for even higher sensitivity and versatility, recently, various gas sensors have also been prepared based on MXene materials, due to the excellent electrical and thermal properties.[54] Composite materials such as CuO/MXene have been prepared to achieve high-sensitivity responses. Other researchers, utilizing the SnO$_2$–TiO$_2$–MXene heterojunction, were able to detect NO$_2$, while MXene/TiO$_2$/MoS$_2$ allowed the detection of ammonia at room temperature. Thanks to these studies, a sensor based on a CuO/TiO$_2$ heterojunction was designed for

19580 | J. Mater. Chem. C, 2025, 13, 19576–19600

This journal is © The Royal Society of Chemistry 2025

ethanol detection, with the addition of conductive MXenes to enhance the sensor's performance.

Considering the continuous decrease in the size of the robots, it is increasingly interesting to find suitable structures for the development of their surfaces. Therefore, the engineering of point defects and the study of the incorporation of single atoms have been explored, which have led to encouraging results. A recent study has used single-atom Cu catalysts on the surface of nanorobots, while further studies have developed systems in which single-atom Pt was used.[55] The different nanorobots have been studied in the capture of microplastics, demonstrating excellent results in this application when illuminated with UV light given by the union of the engineering of point defects and the use of atomic species of Pt. It was also seen that the nanorobots presented a negative photogravitaxis effect and a strong 3D propulsion. Since the development of photocatalytic microrobots, numerous additional semiconductors and materials have been developed with various techniques and applications. By exploiting the two-step synthesis processes of crystalline TiO_2, it has been possible to develop mixtures with different phases and grain sizes, as well as variable external and internal interfaces, thus obtaining various electronic properties.[56] In this study, two types of Co_3O_4 nanomaterials, nanocubes and platelets were integrated with TiO_2 to explore their photocatalytic behaviour. Unlike the Janus structures derived from Co_3O_4 platelets that can develop active swimming thanks to the effective transfer of electrons captured by Co_3O_4 from the TiO_2 band alignment, the Co_3O_4 nanocubes remain isolated from the TiO_2 bands. As a result, there is no band alignment in this case, and these systems do not exhibit active movement under blue light irradiation. By exploiting the deposition of asymmetric Au and Ag layers on $Ti_3C_2T_x$ microparticles, Janus structures with Schottky junctions were developed. When irradiated with UV light, thanks to the presence of an intense electric field inside the structure, the $Au–TiO_2$ microrobots were shown to possess higher speeds due to favourable charge separation and hole accumulation under the gold layer.[57] The researchers also demonstrated that in the presence of 0.1% H_2O_2, even higher speeds could be obtained independently of the UV light trigger, thanks to the silver catalytic properties in H_2O_2 decomposition. These microrobots were also used for pollutant degradation, using polyethylene glycol as a model of polymeric system.
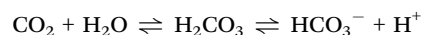
3. ZnO based microrobots

ZnO is a suitable material for water-purification.[58] However, its low colloidal stability in aqueous media typically limits its application in microrobots. A prototypal example consists in catalytically powered Janus microrobots containing two different faces, one of which, the mesoporous ZnO microparticles, was covered with platinum (Pt) used to catalyze the fuel (H_2O_2) decomposition, enabling propulsion.[59] The motion of such mesoporous ZnO/Pt-based Janus microrobots was obtained by bubble propulsion to enable the photodegradation of explosives and dye pollutants.[59] In other examples, light-driven laccase

functionalized ZnO–Au microrobots have been investigated for the synergic destruction of the antibiotic oxytetracycline by enzymatic reaction and photocatalytic activity. In this case, the enzymatic activity of laccase is combined with the photo-induced motion and catalytic degradation of the ZnO–Au microrobots to remove oxytetracycline, one of the most diffused veterinary antibiotics.[60] The ZnO microrobots were prepared by a wet chemistry synthetic approach in which a gold precursor was added during synthesis and laccase physisorption after synthesis led to the formation of microrobots capable of photo-degrading toxic pollutants under UV light, Fig. 3(A) and (B). The speed of a single microrobot was almost doubled by applying UV-light (see Fig. 3(C)). The generation of photo-induced ROS species of the so assembled microrobot in the presence of H_2O_2 fuel permitted the degradation of almost 70% of the pollutant in less than 15 minutes (Fig. 3(D)–(F)).
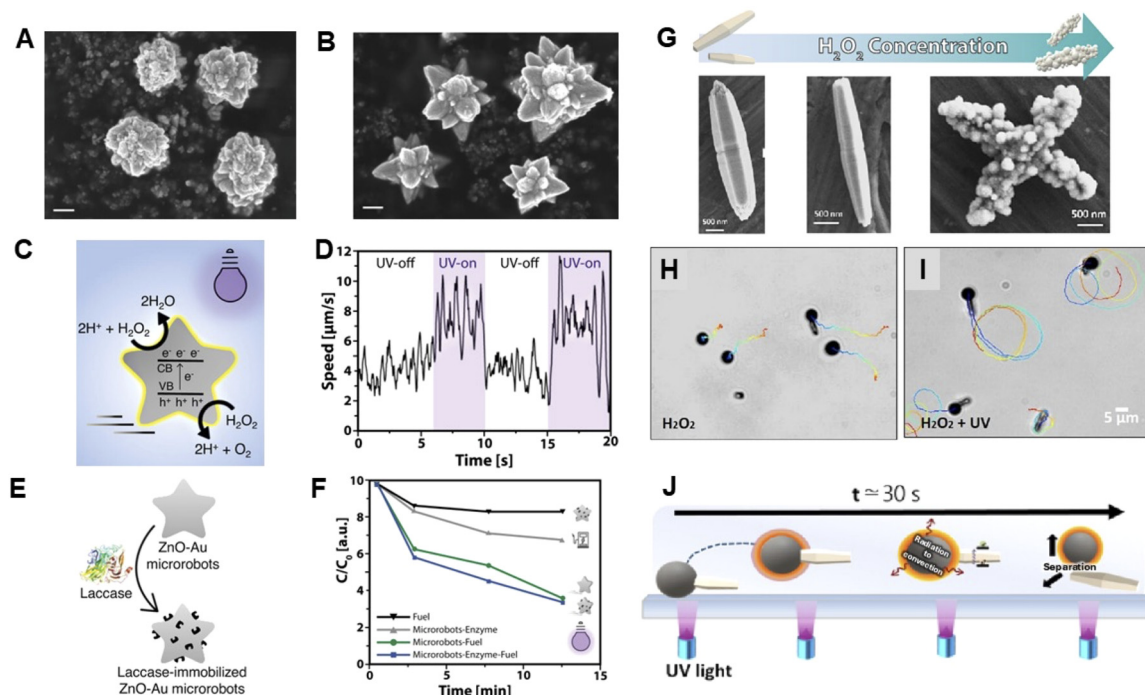
Light-triggered antibiofilm ZnO microrobots have also been designed to destroy biofilms.[62] Biofilms can be defined as complex bacterial communities tightly linked to solid extracellular substrates and are a major source of economic losses, ranging from failures in medical implants to enhanced pipe corrosion in large infrastructures. ZnO microrobot motion and morphology have been optimized through Ag doping. The light-triggered ZnO:Ag microrobot movement is driven by self-electrophoresis. It simultaneously demonstrates antibacterial activity, thanks to the destruction of both Gram-positive and Gram-negative bacterial biofilms from solid surfaces, based on Ag and ZnO synergic bactericidal properties, as well as the autonomous microrobot motion. Synthetic ZnO-based Janus microrobots have been proposed[63] as the first system capable of biomimetic chemotaxis driven by self-reorientation, powered by CO_2 as an alternative biocompatible fuel. Leveraging the excellent biocompatibility of ZnO,[64] microrobots have been designed to actively "'seek out" specific cells or pathogenic microorganisms by chemotactic stimuli (i.e. metabolic CO_2) signals emitted from them and executing targeted biomedical and environmental operations. Building on this concept, Janus ZnO microrod-spherical carbon[61] has been developed, capable of rapid, autonomous self-targeting for bacterial elimination. These microrobots utilize CO_2 as a biocompatible fuel, enabling motion through self-diffusiophoresis driven by ZnO corrosion induced by H_2O_2 fuel (Fig. 3(G)).

The mechanism can be explained as follows. Atmospheric CO_2 is stable and inert in air; in aqueous environments, partial hydration occurs with the formation of carbonic acid (H_2CO_3), which dissociates into HCO_3^- and H^+ ions. The reversibility of the reaction leads to protons (H^+), which are exploited for ZnO-based micromotor (MM) movement. In particular, ZnO reacts with H^+ ions, consuming them and thus shifting the equilibrium to generate more H^+ from dissolved CO_2. This interaction is described by three key reactions:

$$CO_2 + H_2O \rightleftharpoons H_2CO_3 \rightleftharpoons HCO_3^- + H^+$$

$$ZnO + 2H^+ \rightarrow Zn^{2+} + H_2O$$

The released ions – HCO_3^- and Zn^{2+} – have different diffusion coefficients, with HCO_3^- diffusing faster. This generates a local

This journal is © The Royal Society of Chemistry 2025

J. Mater. Chem. C, 2025, 13, 19576–19600 | 19581

Fig. 3 Propulsion mechanisms and functional performance of ZnO-based microrobots. (A) SEM image of ZnO particles and (B) ZnO–Au microrobots, scale bar 500 nm. (C) Schematic representation of the asymmetric production of chemical species during the catalytic reaction of ZnO–Au microrobots in the presence of UV light and H_2O_2. (D) Speed as a function of time of a single micromotor under alternating conditions of UV light on and off, in the presence of 3% H_2O_2. (E) Schematic representation of ZnO–Au microrobots functionalized with the laccase (F) degradation profile of oxytetracycline (model of veterinary antibiotics) (C/C_0) over time, comparing the performance of ZnO–Au microrobots with and without enzymatic enhancement, under UV light irradiation. Adapted with permission from *Small* (Wiley and Sons), ref. 60 Copyright (2022). (G) SEM images illustrating morphological changes in ZnO microrods with increasing H_2O_2 concentrations (0%, 0.625%, and 5%), highlighting the shift from smooth to rough surfaces caused by the development of ZnO_2 crystals; scale bar 500 nm. (H) and (I) Trajectories of microrobots in H_2O_2 (H) and H_2O_2 + UV (I), demonstrating enhanced motion and directionality under UV irradiation, scale bar 5 μm. (J) Schematic representation of UV-induced cargo separation by microrobots after ∼30 seconds, mimicking targeted delivery. Adapted with permission from *Chemical Engineering Science* (Elsevier), ref. 61 Copyright (2024).

field necessary to maintain electroneutrality, creating an electroosmotic movement in the electric double layer on the negatively charged surface of the micromotor, developing the so-called electroosmotic flow. This mechanism results in direct movement towards the ZnO end, and the reaction is based on ambient CO_2 levels in the water. It is believed that the micromotors are chemotactically active towards CO_2, using self-diffusiophoretic propulsion.[63]

External control can guide them to the vicinity of a hidden/uncharted target where they rely on local chemical gradients ([CO_2] or [H^+] gradients) to perform precise chemotaxis (Fig. 3(H) and (I)). The developed ZnO rods were studied as bacteriabots, *i.e.* systems able to mimic the movement of rod-shaped bacteria, such as forward movement, collision, and cargo release. The ZnO rods (about 5 μm long and 1.1 μm wide) were able to move under UV light and H_2O_2 fuel following a mechanism based on photocatalytic water splitting and corrosion of ZnO to ZnO_2. As an example of collision with a passive object, the ZnO rods in an aqueous medium containing 5 wt% of H_2O_2 decreased from about 5 μm s^{-1} to almost 0 μm s^{-1} when it interacted with the carbon microparticle and was recovered to the initial value before the collision (Fig. 3(J)). The systems reported have shown effectiveness for their application as antibiotic agents in biological

environments, a complex goal to address for the several interactions between the biological components and the exogenous agent, that is the microrobot. Indeed, in biological systems, it is crucial to consider the interaction between the micro- and nanostructured materials that constituted the microrobots and the surrounding biological components, which can affect the activity of the photoactive materials, for example through biomolecule absorption or colloidal aggregation in biological media.[65]

4. CuS, Cu$_2$O and SiO$_2$ based microrobots

Binary compounds of copper, such as CuS and Cu_2O, have attracted attention in the biomedical field for their easy fabrication processes and applications in advanced microrobots. A novel approach for the development of biohybrid magnetic helical microrobots that are enhanced with CuS nanodots to improve their photothermal capabilities was presented by D. Gong *et al.* for biomedical applications.[66] More specifically, the CuS-based microrobots were designed for the treatment of cancer cells and pathogenic bacteria. Spirulina, a type of algae with an intrinsic helical structure, was applied as a biotemplate

19582 | *J. Mater. Chem. C*, 2025, **13**, 19576–19600

This journal is © The Royal Society of Chemistry 2025

for the assembly of the microrobots. By integrating CuS nanodots inside the cells and coating them with Fe_3O_4 nanoparticles for magnetic responsiveness, the microrobots achieve effective propulsion and controlled movement in low Reynolds number environments. These microrobots can be guided using external magnetic fields and activated by near-infrared (NIR) laser irradiation at 808 nm, allowing for light conversion into heat. Through this treatment cancer cells and bacteria can be successfully killed. The CuS nanodots enhance the photothermal efficiency of the microrobots, enabling rapid temperature increases sufficient to kill both HeLa cancer cells and *E. coli* bacteria. The study highlights that the microrobots possess high biocompatibility, minor toxicity, and strong photothermal stability, making them viable for reiterate use in the biomedical field. The fabrication process is also cost-effective and facile, making it a scalable option for future applications in drug delivery, minimally invasive surgery, and other therapeutic interventions. In addition, the development of adaptive microrobots made from Cu_2O, a p-type semiconductor with promising properties as a photocatalyst, was explored as well.[67] The Cu_2O microrobots exhibit pH-responsive behavior, switching from negative phototaxis (moving away from the light source) to positive phototaxis (moving toward the light source) as the pH drops below a critical threshold of 4.19. Cu_2O-based microrobots exhibit phototaxis, *i.e.* a directional response to light, which varies based on the pH of the environment. This is desirable for several reasons, including the photoelectric properties of Cu_2O, which is a p-type semiconductor. In the presence of light, electron–hole pairs are generated, and redox reactions are triggered on the surface, which influence the concentration gradient and consequently the self-propulsion force. Depending on the pH, there are variations on the surface, as at pH < 4.19, the protonation of Cu_2O occurs. These reactions can influence the concentration gradient and therefore the self-propulsion force. The variation in the surroundings can cause variations in the propulsion mechanism, varying or even reversing the direction of movement.[67,68]

This feature allows them to autonomously navigate towards a target area, perform their assigned task, such as drug delivery or biomedical intervention, then reverse direction to "evacuate" the area after completion. This level of programmability is significant for biomedical applications, where smart responsive behavior is required. Thus, these microrobots display a novel ability to reverse their phototaxis behavior in response to changes in the local pH of the surrounding environment, making them smart systems responsive to external stimuli. The Cu_2O microrobots were fabricated using a one-pot, template-free hydrothermal approach, which resulted in hollow, cross-linked polyhedral structures. The research demonstrates that these microrobots can precisely follow pre-designed paths and manipulate biological cargo, such as M1 macrophages, under light guidance. Their motion efficiency is also notable, with speeds significantly higher than previously reported Cu_2O-based microrobots. Cu_2O microrobots combined with CdSe nanodots are characterized by a negative phototactic behavior along with a good responsivity to blue light, promoting light-induced propulsion in aqueous
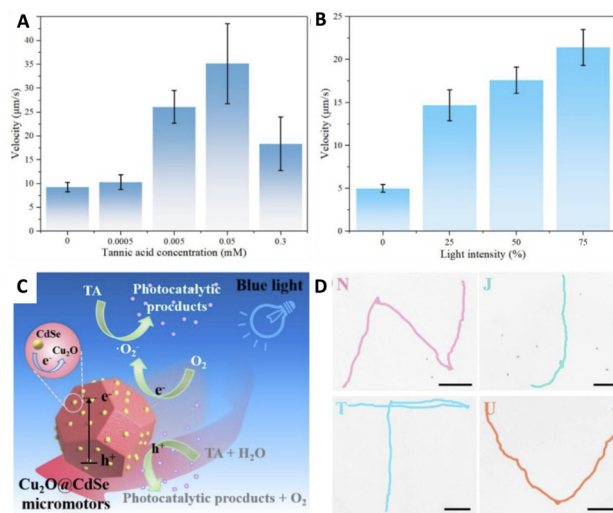

Fig. 4 Characterization of the self-propulsion performance of $Cu_2O@CdSe$ microrobots (5% CdSe QDs) in tannic acid solution, subjected to blue light irradiation. (A) Study of the speed of microrobots by varying the concentrations of tannic acid, with a light intensity of 1.8 W cm^{-2}. (B) Speed of microrobots at 0.005 mM tannic acid according to the intensity of light radiation. (C) Schematic representation of the negative phototaxis mechanism of $Cu_2O@CdSe$ microrobots in the presence of blue light. (D) Trajectories of $Cu_2O@CdSe$ microrobots in a tannic acid solution (0.005 mM), used to write "NJTU" by adjusting the direction of the light source. Scale bars: 20 μm. Reprinted with permission from Applied Materials Today (Elsevier) from ref. 69 Copyright (2021).

solutions containing tannic acid, a molecule that can produce several small molecules (*e.g.* D-glucose and gallic acid) under photooxidation conditions. These small molecules can promote self-diffusionphoresis,[69] reaching speeds as high as ~ 42.3 μm s^{-1} in 0.05 mM tannic acid solution, as shown in Fig. 4.

SiO_2 has been used in the development of microrobots, showing promising results as demonstrated by J. Fu *et al.*[70] The study focuses on the large-scale synthesis of shuttlecock-shaped silica nanoparticles, designed as advanced catalytic nanomotors. These nanoparticles feature a unique asymmetric morphology with a streamlined conical shape with a large opening on one side, which significantly minimizes drag during fluid motion. More specifically, the shuttlecock-shaped silica-based nanoparticles were prepared through a one-pot process using CTAB, SDS, TEA, and TEOS as reagents. The procedure involved stirring, centrifugation, ethanol washing, and calcination at 550 °C. To enable further functionalization, amine modification of these nanoparticles was performed with APTES for further *Candida rugosa lipase* (CRL) immobilization using glutaraldehyde as a linker. This method achieved a CRL loading of 1 mg per mg of nanoparticles. The resulting particles possess a large open cavity that facilitates the efficient encapsulation of the model enzyme lipase, which provides the necessary propulsive force for enhanced catalytic activity. The research demonstrates that these shuttlecock-shaped nanoparticles outperform traditional mesoporous silica nanoparticles, particularly those with a spherical shape, in terms of catalytic performance.

This journal is © The Royal Society of Chemistry 2025

J. Mater. Chem. C, 2025, **13**, 19576–19600 | 19583

5. Magnetic Fe₃O₄-based microrobots

There are some relevant reviews highlighting the high relevance and the potentialities of microrobots based on iron oxides as magnetic components.[71,72] For instance, the innovative development of dual-drive hybrid microrobots was reported, involving a combination of polystyrene and Fe_3O_4, later coated with platinum (PS@Fe₃O₄@Pt) (see Fig. 5).[73] These micro-scale devices can convert ambient energy into mechanical motion. Specifically, they are engineered to utilize two distinct energy sources as chemical reactions and magnetic fields (Fig. 5(A) and (B)). This dual-energy approach not only enhances their efficiency and versatility, but also enables them to execute various tasks such as cargo delivery, environmental cleanup, and biosensing. A key advantage of these hybrid microrobots is their ability to adjust their speed and direction based on the concentration of H_2O_2 fuel and the strength of the magnetic field (Fig. 5(C) and (D)). Such adaptability allows for precise motion control, making them suitable for complex operations at the microscale. Additionally, the integration of multiple energy forms significantly broadens their applications in fields that require high precision and efficiency. An interesting strategy emerging in recent years is the use of magnetically-driven microbubbles as effective tools operating as microrobots to manipulate micro-scale objects.[72] To achieve this, various catalysts, such as platinum, silver, manganese dioxide, titanium dioxide, and cobalt tetroxide, are employed to facilitate hydrogen peroxide decomposition. This reaction produces oxygen, generating bubbles, which can effectively propel microbubbles. Alternatively, Fe_3O_4 can be integrated in order to combine photo-responsiveness along with magnetic features, as in the case of Fe₃O₄@TiO₂/Pt Janus microrobots. When exposed to a low-intensity rotating magnetic field, Fe₃O₄@TiO₂/Pt, Janus microrobots are activated physically. The magnetic rotation

suppresses their rotational Brownian diffusion, while photocatalytic propulsion is achieved via unidirectional irradiation based on a self-electrophoretic mechanism. This process generates a transverse Magnus force. The combination of self-electrophoretic propulsion and the Magnus force, both varying due to magnetic rotation, results in directed motion at an angle from the light direction and enhancing their speed.[74] Further interesting approaches can be designed in order to exploit different physical external stimuli to control the microrobots made of magnetic materials. For example, Fu et al. developed a spiral microrobot equipped with a protective cover, which rotates at 120 rad per s when exposed to a 95 mT magnetic field.[75] They proposed a magnetic drive system that includes a microrobot, a drive system, and a positioning system. The microrobot's motion is controlled by adjusting the magnetic field's frequency and direction, reaching a maximum speed of 2.4 mm s^{-1} at 15 Hz. Several scientists have attempted to combine different coil types to enhance system functionality. The performance of these systems has been tested in microrobot motion experiments, highlighting the potential of integrating magnetic and acoustic drives for complex tasks.

6. Cellulose and organic based microrobots

Organic polymers find applications in fields where inorganic-based materials lack efficiency. In most cases, their contribution goes unnoticed since they are not the principal material. Thus, polymers can be found in advanced functional materials, especially for pharmaceutical products. Of course, they are also used extensively in water purification.[76] Among the organic polymers, cellulose is one of the most abundant organic and polymeric materials in the world. Although humans have been using cellulose since the time of ancient Egyptians, it is only in the last century it was employed as a micro- and nano-material for advanced applications. Thanks to its numerous hydroxyl groups, cellulose could be modified to enhance its physical and chemical properties and to produce hybrid materials, both with inorganic or other organic compounds.[77] In the last year, different cellulose-based materials have been tested for the degradation of organic[78] and inorganic pollutants.[79] The tunable properties of cellulose make it a good host for biosensor applications, also considering its intrinsic advantages. In fact, cellulose is biodegradable, biocompatible, easily available, cost competitive, nontoxic, and renewable. Taking into account these features, cellulose was recently employed in the development of different soft actuators.[80,81]

In general, actuators are mechanical devices capable of producing reversible locomotion, deformations, or changes in properties responding to a variety of external stimuli. Compared to traditional actuators, soft actuators possess lighter, more flexible, and eco-friendly properties as well as good adaptability to multiple environments. Soft microrobots are very useful especially in the biomedical field. In fact, they are adaptable to tissues because they can easily face changes in the
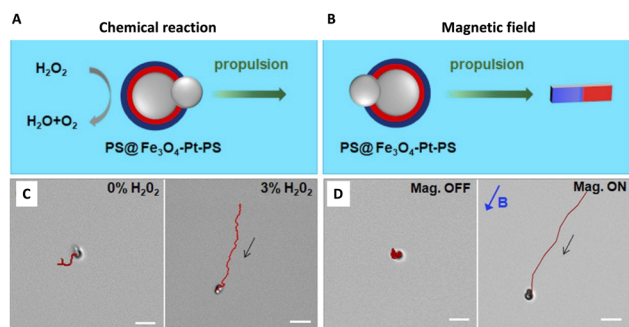
Fig. 5 Motion mechanisms of dual-drive microrobots. (A) Chemical propulsion induced by Pt nanoparticles. The schematic shows the motion of a particle toward the PS end. (B) Schematic of the motion due to the magnetic field; the particles move toward the PS@Fe₃O₄@Pt side. (C) Comparison of micromotor trajectories in two different solutions: in deionized (DI) water (left) and in a 3 v/v% H_2O_2 solution (right). (D) Paths in DI water in the absence of a magnetic field (left) and in the presence of an applied magnetic field (right). The direction of the magnetic field, B, is represented by the blue arrow. The directions of the microrobots are represented by the black arrows in (C) and (D). Scale bar: 2 μm. Reprinted with permission from Colloids and Interface Science Communications (Elsevier) from ref. 73 Copyright (2020).

19584 | J. Mater. Chem. C, 2025, **13**, 19576–19600

This journal is © The Royal Society of Chemistry 2025

fluidic environment of biological systems. Cellulose could be employed as an actuator in the field of soft robotics. Although soft robotics is commonly based on silicone elastomers, urethanes, dielectric elastomer, or reinforced hydrogels,[82] some examples of soft robotics based on cellulose actuators were reported.[83] In particular, soft robotics could be realized with cellulose nanofibers (CNFs), due to their properties like: high strength and flexibility, hydrophilicity, and bio-compatibility,[84] although cellulose nanocrystals (CNCs)[85] and cellulose papers[81] were also successfully employed.

One of the first examples of cellulose-based actuators for biomedical devices was presented in the study of Kim and coworkers for the development of bioartificial muscles based on freeze-dried bacterial cellulose (FDBC) coupled with a conducting layer made with the poly(3,4-ethylenedioxythiophene)-poly(styrenesulfonate) (PEDOT:PSS) co-polymer.[86] FDBC possesses a tridimensional network that can adsorb large amounts of ionic liquids (like EMIM-BF$_4$ and BIMIM-Cl) maintaining at the same time good adhesion strength with the PEDOT:PSS electrodes. This system showed a harmonic response of FDBC hybrid actuators with the two different ionic liquids. The largest bending deformation was obtained by adsorbing EMIM-BF$_4$ on the FDBC actuator and reaching a maximum tip displacement of ± 1.511 mm in the harmonic responses at an input voltage of 3 V, compared to a peak tip displacement of ± 0.711 mm when the ionic liquid was BMIM-Cl.

Cellulose was employed not only in the typical sponge form derived from bacterial cellulose but also as paper to produce multi-responsive actuators. In fact, the same multilayered devices were capable of responding to different external stimuli, such as light and moisture, offering the great advantage in harvesting energy from a variety of external stimuli with only one actuator. Amjadi and Sitti, in 2016, proposed a programmable bilayer actuator based on silver nanowires (AgNWs) and PEDOT:PSS drop-casted on simple copy paper coupled with a polypropylene (PP) film.[87] The driving force was the large hygroscopic contraction of the copy paper united with the large thermal expansion of the PP film. Additionally, an electrothermal activator, a composite material made of AgNWs and PEDOT:PSS, was studied, in order to combine the high electrical conductivity of the former with the high affinity of the latter for paper. The final bilayer functioned with low voltages of less than 8 V, a low input electric power per area of 0.14 W cm^{-2}, and a temperature of less than 35 °C. Under these conditions, they observed a powerful reversible shape-changing behavior with a curvature radius of up to 1.07 cm^{-1} and a bending angle of up to 360°. Furthermore, the fine-tuned actuators tested as soft gripper robots and lightweight wings for aerial robotics produced high output forces and lifted objects 53.7 times heavier than their own weight.[53] These results highlight the potential for practical applications. More recently Nasseri and coauthors, in 2023, reported the synthesis of pH responsive hydrogel nanocomposites by using cellulose nanocrystals (CNCs).[88] The self-healing zwitterionic hydrogel was obtained by co-polymerization of 3-dimethyl (methacryloyloxyethyl) ammonium propanesulfonate (DMAPS) and methacrylic acid (MAA) by a one-step UV-polymerization in the presence of

N,N'-methylenebis(acrylamide) (BIS) as a crosslinker. CNC nanoparticles imparted a liquid crystalline phase and introduced structural anisotropy when added at 10%. The shape-change properties of this hydrogel were investigated at two extreme pH values to expedite actuation, although milder pH conditions could be used to trigger deformation in the biological environment. As a proof-of-concept, they designed two pH-responsive small-scale robots and demonstrated the transport of light cargo using tethered and untethered soft robots made using these hydrogels.

In 2024 Li *et al.* designed a cellulose-based soft robot as a bi-layer structure.[84] They employed an MXene for the design of this material. The top layer is a hydrophilic composite membrane made from a composite (CMN) of cellulose nanofibers (CNFs) used as the matrix, MXene nanosheets as the photoabsorbent, and carbon nanotubes (CNTs) as the conductive cross-linking agent. The bottom layer consists of a hydrophobic Biaxially Oriented Polypropylene (BOPP) membrane, which enables the creation of a flexible bi-directional bending soft robot. Humidity, natural light and electrothermal stimuli can be used to produce fast changes. The obtained soft robots achieved a bending angle of 360° with only 67 mW cm^{-2} of natural light or a voltage as low as 2.8 V, with the corresponding bending curvature of 2.67 cm^{-1}. The fine tunable control of the CMN/BOPP soft robots demonstrated their enhanced applicability in various fields.[89]

Recently, a very interesting example of pollutant removal realized by a soft robotic system was reported[90] by Quin *et al.* In this work, the authors developed a hydrogel-based "bionic fish" capable of dye removal from water with different key properties. It was produced by combining carboxymethyl chitosan (CMC), a modified natural polymer derived from renewable feedstocks,[91] with a poly(*N*-isopropylacrylamide) (PNIPAm) hydrogel. This polymer is capable of solar energy absorption with a hydrophilic/hydrophobic switch at ≈ 32 °C, that is, its low critical solution temperature (LCST). Then, the authors realized the *in situ* growth of Fe$_3$O$_4$ nanoparticles in the cross-linked networks of the PNIPAm/CMC hydrogel. In this way, the fish could be easily removed, thanks to its magnetic properties. This system was able to remove organic pollutants such as Congo red (CR), rhodamine B (RhB), and methylene blue (MB). Furthermore, it filtered out harmful microbes and insoluble particles from a natural lake water and demonstrated remarkable efficacy in salt purification and salt resistance, also after five recycling cycles.

To the best of our knowledge, only recently two studies reported nanorobot systems for water decontamination starting from a cellulose composite. The first one is related to bacterial decontamination. In 2024, a multifunctional MXene composite film was developed incorporating a superhydrophobic Ti$_3$C$_2$T$_x$ MXene nanosheet with bacterial cellulose nanofibers (see Fig. 6).[92] This material shows self-cleaning, photothermal actuation, and photothermal sterilization capabilities. The first step involved rendering the Ti$_3$C$_2$T$_x$ MXene nanosheets superhydrophobic using a mussel-inspired multilayer coating procedure that starts with a polydopamine (PDA) treatment. This PDA-coated MXene, with enhanced ambient stability, was further treated with Ag nanoparticles *via* electroless Ag metallization, and then with a

This journal is © The Royal Society of Chemistry 2025

J. Mater. Chem. C, 2025, **13**, 19576–19600 | **19585**

hydrophobic 1H, 1H, 2H, 2H perfluorodecanethiol (PFDT) coating. Finally, the multifunctional MXene composite film was synthesized by combining superhydrophobic $Ti_3C_2T_x$ MXene nanosheets with bacterial cellulose (BC) using a vacuum filtration process. The self-cleaning properties were successfully tested by demonstrating a water-repellent surface with an impressive water contact angle (WCA) of $152.3 \pm 1.4°$. Furthermore, it displays efficient photothermal conversion performance and stability by reaching a surface temperature over 120 °C when exposed to NIR light. Then, the photothermal actuation properties were successfully tested both in linear and rotational modes, after being exposed to continuous irradiation from a NIR source. The actuator, shaped like an arrow, can advance 5 cm in 11 seconds under irradiation with NIR light ($\lambda = 808$ nm) at an intensity of 0.4 W cm^{-2}. Finally, it also exhibits excellent photothermal sterilization capabilities when tested against typical pathogenic bacteria such as *E. coli* and *S. aureus*. After being exposed to light for 20 min, the MXene/ bacterial cellulose composite demonstrates excellent photothermal antibacterial activities if compared with the control groups, indicating its potential as a promising photothermal material for bioprotection.[58]

Finally, Wang and coworker developed a new composite for conversion of the highly toxic Cr(VI) into Cr(III).[93] In this study, ferrocene (Fc) was combined with cellulose, functionalized with carboxymethyl groups (CMC) and polyethyleneimine (PEI) for Cr(VI) remediation. The driving force is the reversible redox behavior of Fc species and their low ionization potential. The composite with these organic polymers addressed challenges related to conductivity and stability. The hydrophilic groups on the CMC surface allow chelating properties of this material for various metal ions in aqueous solutions. Also, PEI is able to form strong complexing bonds with certain heavy metal ions. Moreover, PEI facilitated the chemical crosslinking and electrostatic interactions of Fc within the CMC, ensuring the good dispersion and stability of Fc. The electrochemical properties of the three-component composite were tested to find a synergistic effect for both the parameters studied. To study the electrochemical activity of the obtained electrode materials linear

sweep voltammetry (LSV) and cyclic voltammetry (CV) analyses were performed, while, to investigate the electrode resistance, electrochemical impedance spectroscopy (EIS) tests were performed. The results were compared with CMC alone and the CMC/PEI combined material. The findings demonstrated electronic and ionic transportation, higher specific capacitance (31.2 F g^{-1}) coupled with improved electrode–electrolyte interactions compared to CMC and CMC/PEI components. The effects of voltage, solution concentration and initial pH on electrochemical adsorption were also investigated. Cr(VI) achieves a maximum fitting adsorption amount of 428.2 mg g^{-1} at an applied electric potential of 1.44 V vs. saturated calomel electrode (SCE) and a reduction rate of Cr(VI) to Cr(III) of 85.4%. This result is 280.5 mg g^{-1} higher compared to those over CMC and CMC/PEI. This material seems to be a potential tool for the complete Cr(VI) removal and detoxification in water treatment.[93] Micro/nanomotors have shown outstanding ability to disrupt contaminants in complex water bodies. New advantages in pollutants removal could be achieved by soft magnetic microrobots technology.

Alongside cellulose, other polymeric soft materials have been used for microrobot fabrication. For example, one system involves 2D carbon nitride-based Janus microrobots based on poly(heptazine imide).[94] When coupling it with the gold-capped side in the presence of H_2O_2 (0.5 vol%) and UV light illumination (1.9 W cm^{-2}, at 365 nm), the robots reached a speed of about 25 μm s^{-1}. The intriguing aspect of this system is that also after illumination for approximately 30 min, the microrobots continue their movement, as a likely consequence of the discharge of stored energy. Chitosan microrobots loaded with Fe_3O_4–ZnO have been used for the efficient photodegradation under the application of an external magnetic field of persistent organic pollutants, using parathion as a model pollutant, degrading it 75% in 30 min,[95] by improving the pollutant transport to the microrobot surface thanks to their speed reaching values as high as 25 μm s^{-1}.

A Janus micromotor combining polycaprolactone as a polymer and PrecirolATO 5 as a lipid led to a soft microrobot propelled by magnetic/IR light movement by combining
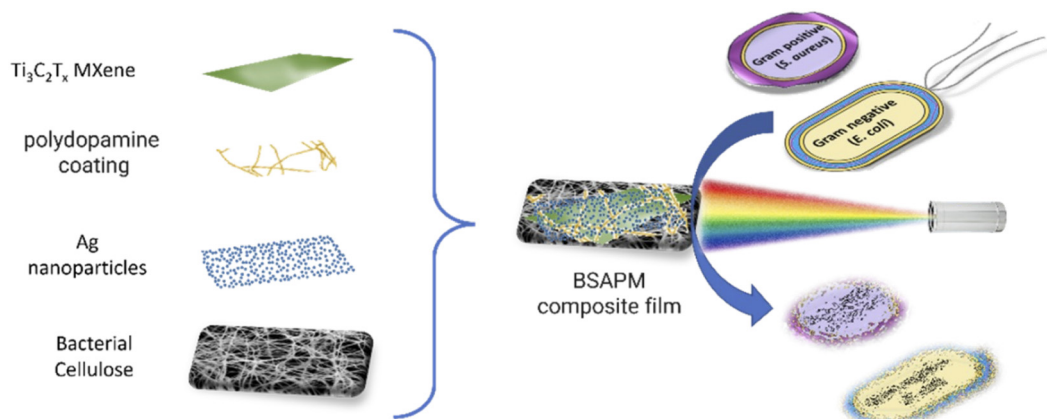

Fig. 6 Schematic representation of the preparation of a BSAPM composite film. Multifunctional MXene composite film based on bacterial cellulose (denoted as BSAPM) with photothermal sterilization capabilities.

19586 | *J. Mater. Chem. C*, 2025, **13**, 19576–19600

This journal is © The Royal Society of Chemistry 2025

polypyrrole nanoparticles (PPNP) and magnetic NPs.[96] These microrobots are shown to induce MB degradation by Fenton-induced reaction. The combination of amine-modified dyna-beads functionalized through EDC/NHS activation with the carboxyl-containing ligand poly(N-[3-(dimethylamino)propyl]-methacrylamide) allows for the fabrication of self-assembling microrobot assemblies.[97] This polymer was chosen thanks to its antibacterial activity. The microrobot assemblies had a plane-like morphology and were able to propel under the action of external magnetic fields. Notably, the speed of the microrobots is dependent upon the size of the assembled plane, reaching values as high as 35 μm s^{-1} for >50 beads in a single assembly. These systems were characterized for their capturing ability of *P. aeruginosa* bacteria and also microplastics under a transversal rotating field of 5 mT and at 10 Hz frequency.[97]

7. Emerging materials for perovskite and chalcogenide-based microrobots

7.1 From bismuth based to perovskite microrobots

Bismuth is able to form almost harmless compounds, earning it the status of a green element. Among these compounds, bismuth oxyiodide (BiOI) is a low bandgap (1.7 eV) photocatalyst, which can be activated by visible light due to its narrow band gap. In a typical example, Dong et al.[98] employed a simple wet chemistry approach to produce BiOI microrobots with one face coated with a metal layer by sputter coating, propelled by the self-electrophoresis mechanism. When exposed to visible light, the electrons from the conduction band are blocked in the metal layer. The H$^+$ ions released from water oxidation move towards the metal layer along with an electroosmotic flow of water molecules to the metal side, causing a net displacement of the particle. This propels the BiOI micromotor with the BiOI side forward with speeds as high as 1.5 μm s^{-1}. When coupled with Fe$_3$O$_4$, Khairudin and coworkers obtained flake-like BiOI–Fe$_3$O$_4$ microrobots able to degrade polystyrene microplastics,[99] reducing their concentration from 0.05 g L^{-1} to 0.018 g L^{-1} under visible light illumination.

BiVO$_4$ also provides many examples given the simplicity of its synthesis and the low resulting bandgap in the visible range, in the interval between 2.3 and 2.5 eV. To this aim, Prof. Pumera's group showed the formation of BiVO$_4$ microrobots capable of capturing bacteria.[100] The non-uniformity of the BiVO$_4$ surface leads to the asymmetrical photogeneration of ions which leads to a net electrical field, generating a symmetry break in the microrobots leading to their self-diffusiophoretic movement. The authors found speeds as high as 5 $\pm$ 1 μm s^{-1} at a very low H$_2$O$_2$ fuel concentration (0.025 wt%). The microrobots could attach *S. cerevisiae* cells and destroy *E. coli* thanks to the photogenerated production of ROS species (HO$^\bullet$, O$_2^{\bullet-}$ and H$_2$O$_2$). The ROS produced by such BiVO$_4$ microrobots are also able to disaggregate protein fibrils,[101] this process being monitored by Thioflavin T fluorescence.

In a different set of works, Heckel and coworkers prepared catalytically active BiVO$_4$ microparticles showing a star-shape morphology with heterogeneous multifacets that can move without asymmetrization.[102] The motion of those microparticles depends on the UV and visible light irradiation, solution pH and zeta potential, reaching speed up to 7 μm s^{-1}. Indeed, the authors observe movement on the side faces for negatively charged particles (pH = 7) and ground-face sliding for positively charged particles (pH = 3). The same authors slightly changed the synthesis conditions to synthesize spheroidal BiVO$_4$ photocatalytic swimmers[103] reaching speeds 3 and 6 μm s^{-1}. They also investigated how these swimmers could form assemblies and the resulting swimming velocities. The formation of composites of graphene oxide with BiVO$_4$ microrobots permits the mimicking of a biomimetic 'predator-bait' behavior,[104] which underpins a competition between the electroosmotic flow and the self-diffusiophoresis. In particular, under low light intensity (0.2 W cm^{-2}) the smaller BiVO$_4$ particles move towards the large-sized 'bait' GO/BiVO$_4$ particles, whereas in the case of higher low light intensity (0.6 W cm^{-2}), the self-diffusiophoresis prevails over the electroosmotic flow and the two particles move away. Interestingly, it is possible to combine a hybrid magnetic and light powered microrobot motion by leveraging Fe$_3$O$_4$@-BiVO$_4$ microrobots to investigate the dynamics of their hybrid motion.[105] The authors found that these microrobots can capture cellulose acetate microplastic fragments derived from cigarette filters by virtue of the opposite zeta potential values. By light-triggered ROS formation in the presence of transversal rotating magnetic field, such microrobots can induce RhB photodegradation, reaching a maximum value of 73 $\pm$ 3% at [H$_2$O$_2$] = 0.1 wt%.

Finally, by leveraging the phenomenal versatility of perovskite based materials, the group of Prof. Pumera showed the fabrication of Bi$_2$WO$_6$ microrobots for textile fiber degradation.[106] The motion of the Bi$_2$WO$_6$ microrobots was characterized by an asymmetrical illumination set-up at low H$_2$O$_2$ concentration (0.025 wt%) reaching 2.9 $\pm$ 0.4 μm s^{-1}. These systems permitted the significant modification of the morphology of textile fibers, as a result of the formation of ROS species under sun-like illumination. It is important to mention that that the inclusion of bismuth in perovskite-based materials avoids the use of harmful lead, thereby achieving more sustainable devices with higher stability under ambient conditions.[107] Remarkably, in the field of microrobotics, to address the poor stability of perovskite materials in water, Wang et al.[108] employed the SU-8 photoresist to stabilize CsPbBr$_3$ nanowires. This approach prevented perovskite degradation in aqueous environments. The authors realized bilayer achiral microrobots by a sequential spin coating approach, in which a bottom Fe$_3$O$_4$ magnetic layer is covered by a top CsPbBr$_3$/SU-8-layer, Fig. 7(A). As a result, these microrobots are actuated by the employment of a magnetic field 3D Helmholtz coil system to roll or navigate on solid surfaces at speeds as high as at 550 $\pm$ 20 μm s^{-1} at 12 mT, as reported in Fig. 7(B).

7.2 Chalcogenide-based microrobots

Besides perovskites, chalcogenide-based microrobots have also been explored for instance by antimony(III) sulfide microrobots.[112]
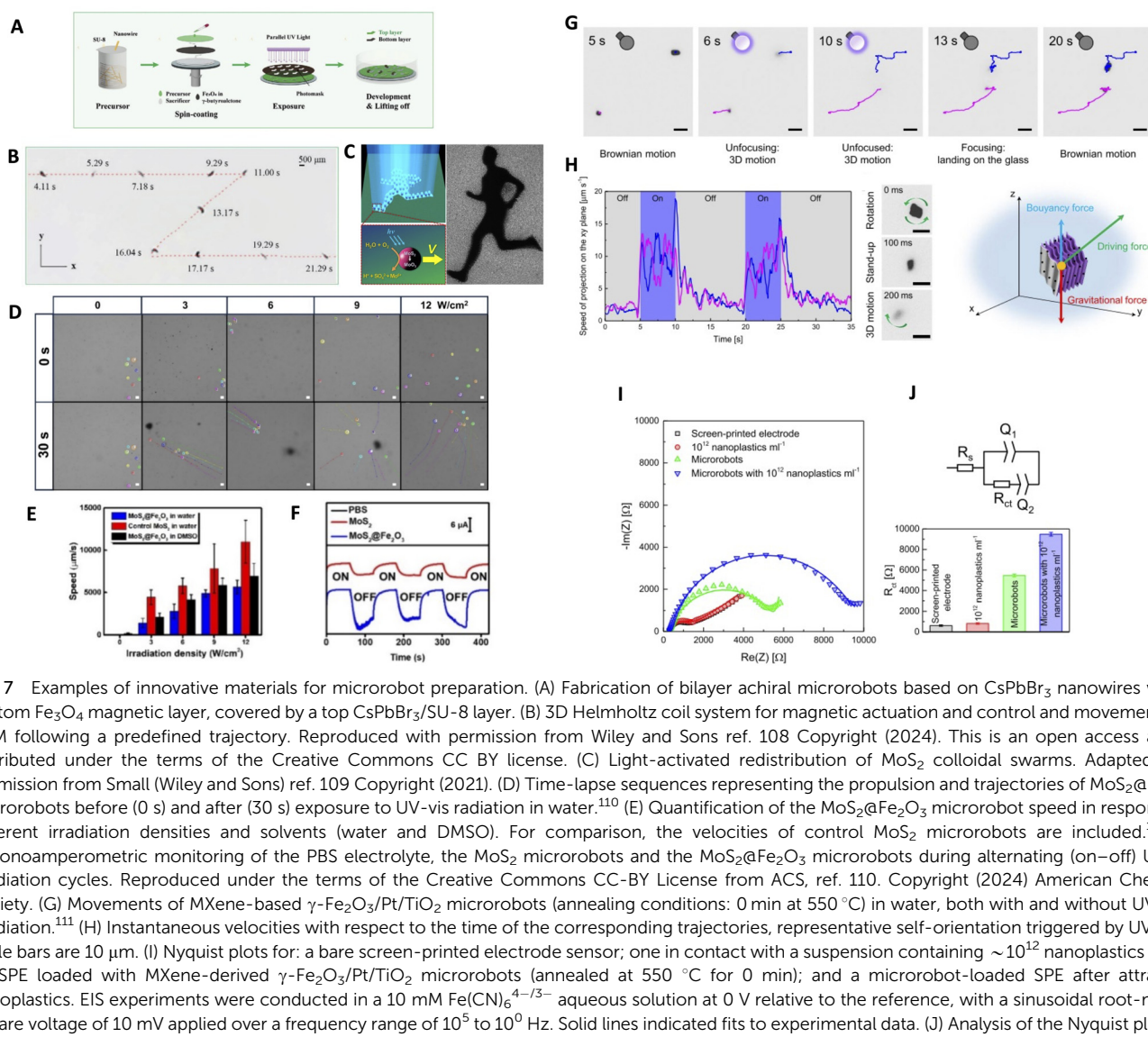
This journal is © The Royal Society of Chemistry 2025

J. Mater. Chem. C, 2025, 13, 19576–19600 | 19587

Fig. 7 Examples of innovative materials for microrobot preparation. (A) Fabrication of bilayer achiral microrobots based on CsPbBr$_3$ nanowires with a bottom Fe$_3$O$_4$ magnetic layer, covered by a top CsPbBr$_3$/SU-8 layer. (B) 3D Helmholtz coil system for magnetic actuation and control and movement of a BAM following a predefined trajectory. Reproduced with permission from Wiley and Sons ref. 108 Copyright (2024). This is an open access article distributed under the terms of the Creative Commons CC BY license. (C) Light-activated redistribution of MoS$_2$ colloidal swarms. Adapted with permission from Small (Wiley and Sons) ref. 109 Copyright (2021). (D) Time-lapse sequences representing the propulsion and trajectories of MoS$_2$@Fe$_2$O$_3$ microrobots before (0 s) and after (30 s) exposure to UV-vis radiation in water.[110] (E) Quantification of the MoS$_2$@Fe$_2$O$_3$ microrobot speed in response to different irradiation densities and solvents (water and DMSO). For comparison, the velocities of control MoS$_2$ microrobots are included.[110] (F) Chronoamperometric monitoring of the PBS electrolyte, the MoS$_2$ microrobots and the MoS$_2$@Fe$_2$O$_3$ microrobots during alternating (on–off) UV-vis irradiation cycles. Reproduced under the terms of the Creative Commons CC-BY License from ACS, ref. 110. Copyright (2024) American Chemical Society. (G) Movements of MXene-based γ-Fe$_2$O$_3$/Pt/TiO$_2$ microrobots (annealing conditions: 0 min at 550 °C) in water, both with and without UV light irradiation.[111] (H) Instantaneous velocities with respect to the time of the corresponding trajectories, representative self-orientation triggered by UV light. Scale bars are 10 μm. (I) Nyquist plots for: a bare screen-printed electrode sensor; one in contact with a suspension containing ∼10^{12} nanoplastics mL^{-1}; an SPE loaded with MXene-derived γ-Fe$_2$O$_3$/Pt/TiO$_2$ microrobots (annealed at 550 °C for 0 min); and a microrobot-loaded SPE after attracting nanoplastics. EIS experiments were conducted in a 10 mM Fe(CN)$_6$$^{4-/3-}$ aqueous solution at 0 V relative to the reference, with a sinusoidal root-mean-square voltage of 10 mV applied over a frequency range of 10^5 to 10^0 Hz. Solid lines indicated fits to experimental data. (J) Analysis of the Nyquist plots by the equivalent circuits: R_s (solution resistance) in series with Q_1 (double layer capacitance), in parallel with R_{ct} (charge transfer resistance) and Q_2 (second constant phase element) and R_{ct} values obtained by fitting Nyquist plots, error bars represent the fit precision. Reproduced under the terms of the Creative Commons CC-BY License from *Nature Communications*, ref. 111 Copyright©(2022).

Interestingly, Sb$_2$S$_3$ is a semiconductor showing low toxicity and sufficient stability in water and air, which can be used with the aim to produce in single pot synthesis in water under microwave heating microrobots that can be moved by employing UV light illumination at a speed of 0.3 ± 0.1 μm s^{-1}, which can be increased up to about 2 μm s^{-1} in the presence of H$_2$O$_2$ fuel at 10 wt%. A thoughtful application of Sb$_2$S$_3$ microrobots has been shown in the field of microplastic degradation.[113] In particular, the photoactive Sb$_2$S$_3$-based microrobots propelled *via* two orthogonal physical modes. Thus, antimony sulfide/ferrite antimony sulfide-based microrobots decorated with magnetite nanoparticles can be designed for poly(3-hydroxybutyrate) and poly(lactic acid) microplastic degradation.[113] The photoactive Sb$_2$S$_3$-based microrobots propelled *via* two independent triggers, magnetic field and light irradiation, which were ultimately enhanced by introducing H$_2$O$_2$ as fuel, reaching a speed of about 1.6 μm s^{-1}. Another remarkable example is constituted by WS$_2$ microrobots, systems able to reach velocities up to 6000 μm s^{-1}.[114]

Of great interest is the MoS$_2$ material, an indirect bandgap (1.23 eV) semiconductor, which has been explored for high speed microrobots. In the seminal paper from Chen *et al.*[109] MoS$_2$ colloidal motors were able to swim in the presence of dissolved oxygen and UV light, triggered by oxygen-induced self-diffusiophoresis. By using structured light, it was even possible to organize the microrobots in two predetermined shapes, as the one of a humanoid runner (see Fig. 7(C)). A phenomenal application of this class of microrobots was shown by their combination with Fe$_2$O$_3$ for microplastic removal,[110] as can be seen in Fig. 7(D). Under full-spectrum solar light irradiation, these systems reached degradation of polystyrene microbeads after four hours, reaching a speed of up to 6 mm s^{-1}, as

19588 | *J. Mater. Chem. C*, 2025, **13**, 19576–19600

This journal is © The Royal Society of Chemistry 2025

reported in Fig. 7(E). The presence of Fe_2O_3 allowed for the easy removal of the microrobots after microplastic degradation. The formation of ROS species was monitored by chronoampero-metric measurements (Fig. 7(F)).

MXenes are metal carbides, nitrides or carbonitrides layered in a two-dimensional material, initially discovered in 2011 by Naguib and co-workers.[89] They are always used in combination with other materials to produce composites with powerful application across various fields.[115] MXene derived oxide microrobots have shown potentiality in the field of nanoplastics collection and electrochemical sensing in aqueous environments. In particular, such microrobots were prepared using $Ti_3C_2T_x$ MXene materials oxidized to multi-layered TiO_2 onto which a Pt layer was deposited and finally loaded with magnetic γ-Fe_2O_3 nanoparticles.[111] As reported in Fig. 7(G) and (H), the microrobot movement is triggered by UV light and consistently leads to speed in the range of 10–15 μm s^{-1}. Interestingly, the authors could demonstrate that owing to the pH-dependent zeta potential of the synthesized microrobots, at pH 3, the microrobots exhibited a negative zeta potential (-60 mV), enabling them to capture nanoplastics with a positive zeta potential at this pH ($+43$ mV) The microrobots' magnetic properties permitted their capture by employing a neodymium magnet. Such captured nanoplastics were subsequently detected by electrochemical impedance spectroscopy using serigraphic electrochemical sensors (Fig. 7(I)–(J)) by measuring the charge transfer resistance (R_{ct}) in a 10 mM $Fe(CN)_6^{4-/3-}$ aqueous solution at 0 V bias with respect to the reference.

# 8. Microrobots in complex environments: from liquid interfaces to biohybrid microrobots

8.1 Liquid–liquid interfaces

The behavior of microrobots is typically studied in aqueous systems or at solid–liquid interfaces, whereas their motility in complex environments, such as dispersions or oil/water interfaces, is still poorly understood, despite many studies in this field having tried to elucidate the exact mechanisms. For instance, it is known that the interface-induced phoresis theoretical model[116] would induce a unique microrobot motion at an interface. Wang et al. proved that at a water–air interface[117] microrobot acceleration is observed due to the smaller viscous drag compared to the liquid–solid interface. Notably, the propulsion in proximity to complex interfaces involving immiscible liquid systems remains less extensively investigated.

To address this gap, our group explored methods for preparing picolitre[118] and femtolitre[119] droplets with precise volume control and investigated the critical role of the reaction confinement at oil–water interfaces at these liquid scales, using inkjet printing technology.[120,121] The question that can arise within the context of microrobots is the following: can an oil–water interface modify their movement mechanism? The experiments of Liu et al.[122] demonstrated chemical reactions powering a micromotor at a silicone oil–water interface, leading to a significant increase

(typically in the range between 3 and 6 fold) in motor speeds, as reported in Fig. 8(A). The microrobots they tested were formed employing previously reported fabrication assemblies and were characterized by Janus-like geometries, such as SiO_2–Pt, PS–Pt, TiO_2–Pt, WO_3–Pt, and Au–Pt types and PS–Ni–Pt Janus SiO_2–PtO Janus structures (Fig. 8(B)). These were typically prepared by sputtering or metal evaporation on microbeads. The authors wisely analyzed the possible reasons for such increase in microrobot speed (Fig. 8(C) and (D)), such as tilt angles (i.e. the angle formed between the plane that divides the two caps of a Janus microrobot and the surface onto which it floats), hydrodynamic slips, interfacial permeability, electroosmosis, and surface tension gradients, finding that these effects play a quantitatively little effect on the observed speed increase. The reason for such improvement is likely speculated to be of electrostatic origin, due to charges confined at the oil–water or air–water interface, as a result related to electrical field induced acceleration of chemical reactions in microdroplets.[123,124]

In a similar paper, Arlasnova et al. prepared Pt/Au rods to study their motion at the interface between hydrogen aqueous peroxide solution and n-decane,[125] observing a significant increase of the speed, up to 8 fold higher than their velocities near a solid wall. Accordingly, the enhancement in velocity is tentatively explained by the authors as due to electrokinetic effects and the position of the rods at the water/oil interface. Albeit plausible, this effect still requires careful demonstration. To this end more experiments are necessary, especially to understand the possible crucial role of microdroplet confinements at lower volume scales. An insightful application in the
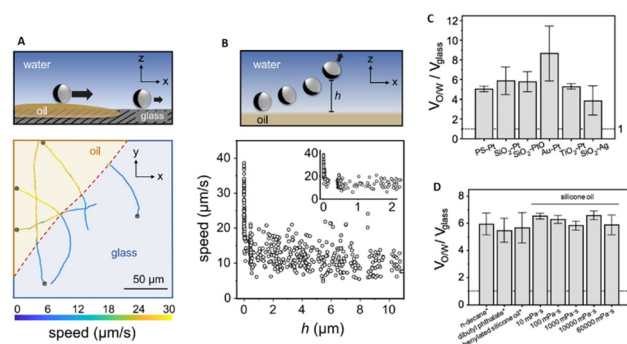
Fig. 8 Illustration of the increased speed of microrobots at oil–water interfaces. (A) Scheme (top) and real (bottom) trajectories of 5 μm PS–Pt microrobots, during the movement from the glass surface of a glass towards a silicone oil–water interface. The boundary line of the oil drop is represented by the dashed line. The instantaneous motor velocities are represented by a color code. (B) Velocity diagram of 5 μm PS–Pt microrobots (top, schematic; bottom, instantaneous) during movement from a silicone oil–water interface to bulk water. The upward movement is probably due to a heavier Pt plug oriented toward the bottom. The experiments were all performed in 5 wt% H_2O_2. Increased microrobot speeds at oil–water interfaces for different motor types (C) and interfaces with different oils (D). $V_{o/w}$ and V_{glass} are the microrobot speeds at the oil–water interface and on the glass surface, respectively. The reported error bars are the standard deviation calculated on more than 200 microrobots. Reprinted with permission from Liu et al. ref. 122 (ACS) Copyright©2024, American Chemical Society.

This journal is © The Royal Society of Chemistry 2025

J. Mater. Chem. C, 2025, **13**, 19576–19600 | **19589**

field of microrobot intervention within complex environments (*i.e.* sand–water system) is provided by the work of Liu and coworkers,[126] who prepared N-UiO-66 MOFs by high-gravity technology. Subsequently, the N-UiO-66 MOFs were assembled onto polystyrene microbeads and asymmetrically loaded with MnO$_2$ that allowed for ultrahigh speed in the presence of 5% H$_2$O$_2$ fuel (1135 μm s^{-1}). The resulting microrobots were found to easily diffuse through a water–sand–water system and improve the adsorption capacity of methyl orange dye by approximately five times with respect to the initial MOF system.
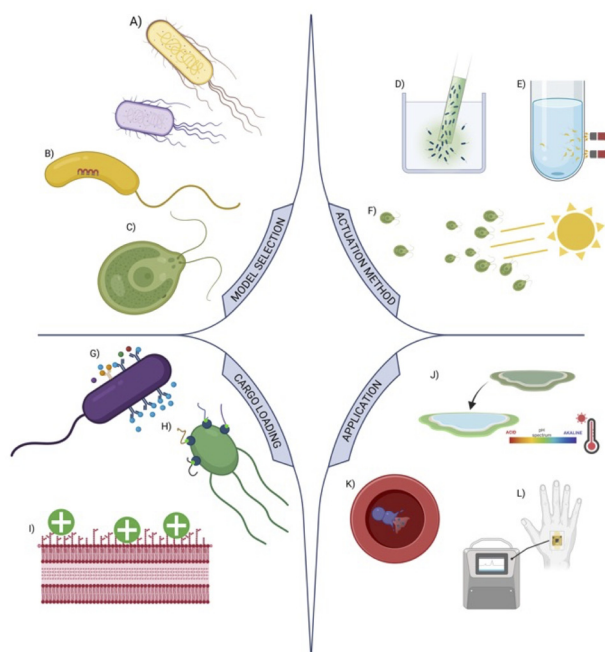
8.2 Biohybrid microrobots

Microorganisms can be harnessed as ''biohybrid'' microrobots, exploiting some cellular characteristics. Current in-development models make use of some microalgae species, mainly *Chlamidiomonas reinhardtii*,[127,128] or flagellated bacterial species such as, but not limited to, *Serratia marcescens* or *Escherichia coli*.[129] These biohybrid microrobots (see Fig. 9) leverage the intrinsic motility of microorganisms as propulsion, or actuation, due to their natural capability to perform simple movements following chemotactic, phototactic or magnetotactic stimuli, enhancing their ability to perform complex tasks autonomously in dynamic environments.[130,131] The anchorage of the microorganism to the carrier support may also happen through aspecific interactions,

Fig. 9 Main features of biohybrid microrobots. Graphical representation of the key aspects of microbial biohybrid nanorobot technology. The most commonly used models are bacteria, *E. coli* or *S. marcescens* (A), *Magnetospirillum* spp (B), or microalgae, *C. reinhardtii* (C). Actuation methods can rely on chemotaxis (D), magnetotaxis (E) or phototaxis (F). Loading of the cargo may happen through specific interactions, such as antigen–antibody (G) or biotin–streptavidin (H) binding, or through aspecific interaction, based on charge attraction (I). Field applications may range from environmental remediation and sensing (J), drug delivery (K) or diagnostic biosensors (L). Created with **https://BioRender.com**.

such as positively charged polystyrene beads that can interact with the negatively charged outer membrane of *S. marcescens*, thus allowing the bacteria to displace the beads.[132] Alternatively, this may happen *via* specific affinity-based mechanisms, such as biotin–streptavidin, or antibody–antigen binding.[133] Moreover, the implementation of modern molecular and synthetic biology approaches allows researchers to expand the biological capabilities of these biohybrid microrobots. For instance recombinant DNA technology can be used to enable microorganisms to produce the cargo themselves, or enhance specific native pathways, tailoring the microorganism to its intended role.[134,135]

Advancements in biohybrid microrobot technology focus on enhancing the functionality and applications of biohybrid microrobots in various fields. Current actuation methods are based on the natural capability of certain microorganisms to navigate in the environment by responding to different types of stimuli: light sources for phototactic organisms, different chemicals for chemiotaxis, and magnetic fields for magnetotaxis, with each of these having its own advantages and limitations.[136] *C. reinhardtii*-derived microrobots can be easily modified with optical stimuli, thanks to the natural phototactic capability of the algae, thus not requiring additional modifications. The phototactic response is rapid (response time is on the order of seconds), precise and modulable, since the microorganism response varies according to the applied intensity.[137] Limitations may occur in closed environments, such as deeper tissues of the human body, considering that light might not be able to reach them, and the usage of UV or infrared light might induce cellular damage.[138] Chemotactic actuation is another versatile approach because many motile bacteria express various types of chemoreceptors, being able to move towards or against an impressive variety of chemicals. Nevertheless, it is limited by several conditions: firstly, the microorganism must express the appropriate receptor to recognize the molecule of interest; secondly, directing the microrobot is slow and heavily dependent on the chemical concentration; lastly, chemotactic movement is limited to aqueous media.[138]

Magnetic-based control is rapid and versatile in accessing diverse environments and can be implemented using naturally magnetotactic species such as *Magnetospirillum gryphiswaldense* or *Magnetospirillum magneticum*, or appropriately modified models. As discussed previously, even this method has its limitations: it requires an external stimulation system and electromagnets may overheat the target system. Also, similarly to non-phototrophic species, non-magnetotactic microorganisms must be previously adapted and engineered for them to be viable.[139,140]

Microbial microrobots can find various applications. For instance, they are capable of real-time monitoring of pollutants in water and soil, utilizing their natural motility and chemotactic responses to navigate toward contaminants. These microrobots can also be engineered to detect specific toxic substances and respond accordingly, thereby enhancing efforts in pollution control and removal.[141] Additionally, they can facilitate *in situ* sensing of biochemical parameters, such as pH and temperature, providing valuable data for environmental assessments.

19590 | *J. Mater. Chem. C*, 2025, **13**, 19576–19600

This journal is © The Royal Society of Chemistry 2025

Their ability to operate autonomously in challenging environments makes them promising tools for sustainable environmental management.[48,142] Biohybrid magnetic algae robots (MARs) based on *Chlorella vulgaris* (*C. vulgaris*) leverage the magnetic features of Fe_3O_4 nanoparticles allowing for precise movement at the average speed of 7.5 μm s^{-1} under a rotating magnetic field at 3 mT intensity and 50 Hz frequency.[34] These systems were able to capture and remove 50 nm diameter amino-modified polystyrene beads – nanoplastics (80% removal efficiency) and remove 1.5 μm diameter amino-modified polystyrene beads – microplastics (54% removal efficacy) through electrostatic interactions. In the biomedical field, they can facilitate targeted drug delivery, navigate through body tissues, and perform minimally invasive surgeries by mimicking the movement of immune cells.[143,144]

8.3 Perspectives of microrobots in water remediation: advantages and challenges

Today, the most traditional approaches used for water treatment can be resumed by considering sedimentation, filtration, adsorption and photo-electrochemistry processes.[145] On the other hand, use of microrobots is emerging as a promising approach in the field of water treatment due to their ability to actively navigate and interact with contaminants at the microscale, offering targeted removal of heavy metals, dyes, and pathogens.[146] Owing to their active motion, self-propelled programmable micro- and nanoscale synthetic robots provide exciting opportunities to improve water monitoring and remediation processes, enhancing treatment efficiency by overcoming diffusion-limited reactions and promoting interactions with target pollutants.

Interestingly, the most important parameters concerning the use of MNRs in water purification involve environmental compatibility and operational feasibility. Technically, they must be able to move efficiently in water, selectively target specific pollutants, and remove them effectively through adsorption, degradation, or catalytic reactions. They should also be designed to either degrade safely or be easily retrieved to reuse or prevent secondary contamination. From an environmental point of view, the materials used must be non-toxic and safe for the aquatic life. The microrobots should remain stable and effective under various real-world water conditions, such as changes in pH, salinity, and temperature, while minimizing their ecological impact over time.

On the other hand, the effectiveness of microrobots in pollutant degradation is influenced by the concentration of pollutants, the presence of interfering species, the concentration of nanomotors, and the contact time. It is known that high pollutant concentrations may lead to surface saturation, reducing removal efficiency.[147] Moreover, interfering species such as competing ions or organic matter can hinder microrobot activity by blocking active sites or affecting motion behaviour.[148] To minimize these effects, the concentration of microrobots must be optimized to ensure sufficient pollutant interaction while minimizing cost and environmental impacts.[149] Moreover, contact time directly affects the degradation or adsorption rate, where prolonged exposure improves remediation efficiency up to a point of equilibrium.

Considering the most remarkable reports on MNR-driven pollutant degradation analysed in this review, it is possible to observe that in the common protocols the tested materials are studied under specific experimental conditions. The MNR concentration is typically on the order of a few mg mL^{-1}, significantly in excess with respect to the pollutant concentration which is on the order of 10^{-2}–10^{-5} M. After an initial period needed to obtain pollutant-MNR adsorption–desorption equilibrium, the system is subjected to the intended combined stimuli (*e.g.* light irradiation and magnetic field) in a kinetics study typically on the order of tens of minutes to ensure almost complete pollutant degradation. Control experiments are usually carried out in the absence of stimuli, in the absence of MNRs to characterize the photolysis of the pollutant or, when conducting photo-degradation of the pollutant, in the presence of non-motile yet photocatalytic microsystems to demonstrate the superior ability of MNRs in photodegradation given their self-propulsion ability.[48] Notably, only in a few reports the MNRs are reused after a few cycles of use,[50,69] finding that the MNRs retain their functionality. As far as the interfering species are concerned, the crucial role of ions in the fluids where the microrobots are immersed has been investigated[150] and also theoretically analyzed.[151] The motion of MNRs is based on the formation of the electric fields between the charged MNRs and the Debye layer, whose size can be dramatically influenced by the ionic strength of the surrounding fluid, hence decreasing the MNR mobility. Finally, to better understand the photodegradation mechanism of the pollutants, the research studies typically take into account the role of photocatalytic species $^{\bullet}O^{2-}$, h^+, and $^{\bullet}OH$, using specific scavengers such as benzoquinone, ethylenediaminetetraacetic acid and isopropanol,[27,48] finding the most plausible species that govern the degradation of the pollutant whilst quantifying the role of possible interferences that could affect the MNR activity in complex fluids.

However, despite their potential, there are several limitations that currently prevent them from being deployed on a large scale, most notably scalability. Indeed, while microrobots can be considered effective in laboratory settings, the deployment of microrobots in large water bodies or treatment plants remains impractical. In fact, microrobots must be collected after treatment to prevent secondary contamination; yet, current recovery methods are inefficient. To improve applied research in the field of water treatment, two main strategies would ideally be appropriate. The first strategy would be to develop new separation technologies capable of effectively and efficiently removing micro/nanoparticles after water treatment processes. The second strategy would be to consider the approach of using micro- to macroscale systems, applying the principles of water treatment by microrobot research at the lab scale. In this context, Barreca *et al.* have designed the innovative "up-and-down" adsorption process recently proposed for pyrene removal from acidic wastewater.[152] This active behaviour significantly enhances mass transfer and accelerates reaction kinetics, enabling faster and more efficient removal of contaminants. Looking forward, microrobotic water remediation lies in the integration of technologies and sustainable

This journal is © The Royal Society of Chemistry 2025

J. Mater. Chem. C, 2025, **13**, 19576–19600 | **19591**

design principles. Sensor equipped microrobots could dynamically adapt their behavior based on contaminant concentrations or environmental cues, optimizing their performance in real time. Environmentally friendly and biodegradable materials will be essential to minimize the environmental impact and ensure that the microrobots themselves do not become pollutants. It is true that this technology is still at an early stage of development, but several studies have highlighted its potential, particularly in the removal of emerging contaminants such as micro- and nanoplastics. The ability to operate at the nanoscale allows micro/nanorobots to interact with pollutants in a highly specific manner, achieving a level of precision that conventional methods such as filtration, precipitation, or adsorption generally cannot reach. Furthermore, their autonomous motion enables them to navigate complex environments and access areas that are often unreachable by passive materials.

Intriguingly, use of micro/nanorobots can have promising prospects as a new type of water purification method, considering that research in this field is still in its early stages and their practical application in wastewater treatment faces significant challenges. Issues such as limited scalability, high costs, environmental compatibility, and the current reliance on chemical fuels are well recognized in the literature. For these reasons, micro/nanorobots cannot yet compete with more established technologies like adsorbents or photocatalysts in terms of large-scale water remediation. To date, research on micro/nanoplastic elimination by micro/nanorobots is still in the laboratory stage; therefore, the transfer to real systems is a crucial challenge that needs to be addressed. Researchers should improve and optimize the stability, recyclability and biocompatibility of micro/nanorobots.

The advantages of microrobots compared to heterogeneous catalysis are several and can be applied in different fields, as follows. Microrobots can move in the reaction medium unlike classical catalysts that are added passively to the medium, their movement facilitating the possibility of reaction between the reagents and the catalyst, unlike classical catalysis that requires mechanical agitation. They are easily and dynamically controllable thanks to external stimuli such as light or magnetic field, unlike classical catalysis that requires more rigid control, being

potentially used in complex environments and thanks to their magnetic or selective properties they can be easily recovered and reused. Last but not least, they can have specific targets and therefore applications also in the biomedical field, which classical catalysis lacks.[55,153,154]

9. Conclusions and perspectives

This review aims at providing the reader with an overview of the materials science involved in microrobot fabrication advancing the research on pollutant decontamination. The evolution of materials design has permitted the researchers to combine sustainability and reconfigurability in synthesis approaches along with low fuel consumption. To facilitate the wider adoption of microrobots in science and technology, the shift from magnetic to light or chemical controlled motion might be a tremendous advantage. Of great interest is the implementation of solar-driven photocatalytic microrobots, which have demonstrated superior speeds in comparison to conventional UV light driven systems and can be combined with fuels to further enhance their performances.

In our opinion, three new forefront perspectives will likely permit this research field to expand and become active matter of new investigations in the materials science community advancing the established technologies for pollutant decontamination: microrobot synthesis, behaviour in complex media and bioinspired communication strategies (see Table 2).

The first perspective deals with the sustainable synthesis of microrobots by rational and scalable strategies that are also cost-effective. Notably, photocatalytic and magnetic composite materials are the most explored for light or magnetic field triggered motion. Single-component photocatalytic microrobots are typically synthesized by chemical methods such as hydrothermal reactions, sol–gel, and coprecipitation. These methods offer advantages and allow for higher yields compared to vapor deposition or sputtering techniques. The earliest photocatalytic microrobots were sensitive only to UV light, making it necessary to design microrobots capable of utilizing visible radiation as well. Metal-free microrobots based on C_3N_4 have been developed,

Table 2 Overview of the specifications of MNRs for applications in environmental decontamination

Application	Prerequisite	Advantages with respect to established technologies	Perspectives
Synthesis scale-up and low-energy low fuel consumption	Multi-material designs and high-throughput production combining different materials by additive manufacturing	Enhanced pollutant decontamination efficiency given the reconfigurable combination of multiple stimuli (light, magnetic, chemical)	Materiomics-based design for reconfigurable motion Dual or even multi-mode microrobots Fuel-free operation
Locomotion control in complex media and recovery	Adaptable motion behavior with sufficient speed in high viscosity media or at the interface with immiscible interfaces	Spatial control in pollutant detection, transport and removal from selected areas	Integrated locomotion control Understanding the physical chemistry of microrobot motion in complex environments Recovery strategies after use
Collective behaviour for remote intervention	Microrobot stability balanced with good biodegradability, absence of toxic products formed after their motion	Time-dependent control of microrobot migration under external stimuli permitting adaptive and robust action	Use of machine learning in controlling microrobot operation Realization of intelligent microrobots through programming intervention

19592 | *J. Mater. Chem. C*, 2025, **13**, 19576–19600

This journal is © The Royal Society of Chemistry 2025

finding significant applications in environmental fields, as they can capture heavy metals in solutions through acid–base interactions between their surface and the metal. Another material that enables the use of visible light is $BiVO_4$, which also demonstrates good photostability. This type of micromotor has been used in various applications, such as preventing microbial contamination, oxidizing benzylamine, and degrading organic pollutants. Single-component microrobots have shown several fabrication advantages. However, their use has been limited by the need for fuel to achieve propulsion and their dependence on specific types of radiation. Their high speeds in pure water have made the use of heterojunction microrobots advantageous compared to single-component ones. The first ones studied were those based on TiO_2/Au, followed by Cu_2O/Au, Si/Au, Fe_2O_3/Au, $BiOI/Au$, ZnO/Pt, C_3N_4/Pt, and $AgCl/Ag$. However, even in these cases, limitations stemmed from the need to use chemical fuels or organic solvents to enhance propulsion. Metal–semiconductor heterojunctions permit self-propulsion in aqueous environments even at low illumination, allowing for applications in various fields. Nonetheless, the low yield of the micromotor, high costs, and lengthy fabrication processes have hindered their broader development. The use of low-cost metals or metal alloys could provide a solution to these challenges. Another strategy to address the limitations of the previously mentioned structures is the development of microrobots that incorporate two semiconductors within their structure, ultimately facilitating the charge transfer between materials.

Large-scale applications of micro- and nanorobots are severely constrained by natural, technological, and economic challenges. A major limitation lies in their industrial-scale fabrication, as most published studies still rely on low-scalability, laboratory-based experimental approaches.[155] The transition to mass production could be facilitated by advanced techniques such as scalable photolithography[156] and additive manufacturing,[157] which enable the fabrication of high-resolution microrobots with complex geometries. In particular, 3D printing stands out as a promising solution due to its versatility in assembling multi-material designs and its capacity for high-throughput production.[12] Another significant challenge is the reliance on chemical fuels for propulsion. Hydrogen peroxide, although widely used, poses safety concerns at concentrations above 3 wt%, thereby limiting its deployment in open or natural environments. To address this, several biocompatible alternatives are being investigated, including urea, glucose,[155] or even water, particularly when propulsion occurs in aqueous media.[158]

To overcome the drawbacks associated with chemical fuels, fuel-free propulsion strategies are under active development. These rely on external physical stimuli, such as magnetic or electric fields, light irradiation, or ultrasound, to induce and control microrobotic motion.[159] However, despite their promise, the practical implementation of such systems in real-world environments, such as open water or contaminated soil, remains technically demanding, largely due to the need for adaptability to fluctuating environmental conditions. In this context, recent advances have demonstrated innovative approaches aimed at enhancing micromotor stability and control under harsh conditions. For instance, Cu_2O-based micromotors have shown responsiveness to pH variations;[67] Fe-doped $g-C_2N_2$ has maintained functionality in highly alkaline environments;[160] and Pt/polyaniline-functionalized TiO_2 microspheres have been shown to operate effectively in saline media up to 0.1 M NaCl.[161] Despite the significant progress achieved, further studies are needed to fully address these challenges. Promising directions include leveraging the dynamic reconfigurability of these systems[6] and employing machine learning-assisted design strategies,[162] with the goal of enabling fully functional microrobots capable of operating under complex and variable environmental conditions.

As perspectives, new systems based on water stable perovskites could highlight the future design of new microrobots, given the extraordinary optical and electrical properties of these materials. In addition, carefully designed experimental design strategies enable the optimization of synthetic schemes, enhancing morphology control and photocatalytic efficiency of the microcrystals by reducing the number of involved experiments. Secondly, the use of well-established 3D printing methodologies[12] allows for the reduction of fabrication costs along with standardization of the size, geometry, composition and scalability. Within real-world harsh environments, the colloidal stability and the reusability of microrobots must be carefully engineered, by optimizing the material composition and tuning the external stimuli or the reaction conditions. Since most of these experiments are conducted in aqueous environments, the degradability and pollutant adsorption capability of the microrobots is an important but still underexplored aspect, which deserves future investigations.

A second aspect of fundamental importance is the investigation of microrobot functionality and motion in confined environments and liquid–liquid interfaces. This is a fundamental science question but also has many important consequences for environmental related microrobot functionality. Indeed, the functionality of microrobots in complex media is still an open question, since it is not completely clear what mechanisms underpin their movement in heterogeneous liquids or in liquid–liquid interfaces where phase separation, electrostatic and surface gradient effects play a role. Many efforts have shown that the reduction of viscous drag can greatly influence the movement of microrobots; however, it can be expected that further research is needed to decipher the role of liquid–liquid phase separation in controlling the position and orientation of microrobots. It is known that confinement in such complex environments might lead to a different reaction kinetics, due to a complex interplay of solvation, molecular crowding and reduced diffusion distances, mimicking the conditions of living cells. Understanding the control of microrobot motion in an intrinsically heterogeneous ambient, which is far from equilibrium,[163] could perhaps become a strategy for improving the sustained motion of microrobots and ultimately making them usable for decontamination in complex environments.

Apart from the basic science point of view, confinement can provide a useful method for prompt microrobot usage and recovery. Indeed, to optimize the performances of magnetic micro-/nano-robots (MNRs) as well as to limit their effect (themselves ''pollutants'') on aquatic matrices, the aforementioned devices

This journal is © The Royal Society of Chemistry 2025

J. Mater. Chem. C, 2025, 13, 19576–19600 | 19593

must be recovered, for example, after having eliminated heavy metals from the water, by different methods such as magnetic, photoinduced and membrane separation. Subsequently, heavy metals can be desorbed by chemical–physical methods allowing their reuse.[164–166] It is clear that the examples herein provided represent a proof-of principle demonstration of the functionality MNRs without a clear description of their recovery after usage. However, apart from the possibility to recover the MNRs by external magnetic fields, a remarkable advancement was shown by Vilela *et al.*,[167] in which the authors leveraged the porous structure of polyurethane-based sponge in which cobalt ferrite microrobots were dispersed within to facilitate the capture of pollutants and also the recovery and reuse of the MNRs. The authors investigated the reusability of such MNRs by the catalytic degradation of malachite green dye in the presence of H_2O_2 concentrations by five consecutive cycles retaining 60% of the decontamination ability.

A third remarkable advancement consists in the communication strategies that can be programmed among microrobots to enhance their capabilities in complex and dynamic scenarios of intervention. This aspect is still far from being fully demonstrated, in comparison to typical microrobots produced by mechatronics.[21] Some studies have demonstrated microrobot communication in the form of magnetic driven motion,[168] eventually leading to globally controlled motions.[169] An advancement in microrobot motion under the magnetic field has been recently shown by the implementation of advanced machine learning approaches, namely reinforcement learning[170] or multiagent reinforcement learning.[171] Despite being constructed from diverse materials—ranging from light-responsive semiconductors like TiO_2, to magnetic hybrids, biodegradable hydrogels, and even biohybrid components—all these microrobots share key functional traits. They are designed to be stimuli-responsive, meaning they can sense and react to specific environmental cues such as light, magnetic fields, or the presence of pollutants. This responsiveness enables precise movement and targeted action in contaminated environments. Additionally, they all aim to degrade or remove pollutants efficiently, often through catalytic processes or physical entrapment. Another shared goal is environmental compatibility: many are made from biodegradable or eco-safe materials to minimize secondary pollution. Ultimately, these microrobots represent a fusion of advanced materials science and robotics, working toward a common purpose—smart, adaptive, and sustainable environmental decontamination.

In conclusion, further research in the microrobot sector will need an interdisciplinary effort, given the enormous possibilities and applications in so many different fields. In this scenario, the role of materials scientists is clearly focused on the continuous evolution of sustainable and intelligent materials design applicable in real world scenarios.

Author contributions

Silvia Orecchio: writing – review and editing, writing – original draft, visualization, validation; Giuseppe Arrabito: writing – review and editing, writing – original draft, visualization, validation, project administration, methodology, funding acquisition, conceptualization; Claudia Pellerito: writing – review and editing, writing – original draft, visualization; Tiziana Fiore: writing – review and editing, visualization, validation; Floriana Campanile: writing – review and editing, writing – original draft, visualization, validation; Federica Meringolo: writing – review and editing, writing – original draft, visualization, validation; Paola Costanzo: writing – review and editing, writing – original draft, visualization, validation; Sebastiano Alberto Fortuna: writing – review and editing, writing – original draft, visualization, validation; Salvatore Barreca: writing – review and editing; Giorgia Puleo: writing – review and editing, visualization, validation; Vittorio Ferrara: writing – review and editing, writing – original draft, visualization, validation, methodology, investigation, data curation; Bruno Pignataro: writing – review and editing, supervision, resources, project administration, funding acquisition.

Conflicts of interest

There are no conflicts to declare.

Data availability

No primary research results, software or code have been included, and no new data were generated or analysed as part of this review.

Acknowledgements

19594 | *J. Mater. Chem. C*, 2025, **13**, 19576–19600

This journal is © The Royal Society of Chemistry 2025

Notes and references

1 M. K. Kardos, M. Patziger, Z. Jolánkai and A. Clement, The new urban wastewater treatment directive from the perspective of the receiving rivers' quality, *Environ. Sci. Eur.*, 2025, **37**(10), 10.

2 D. Lascari, S. Cataldo, N. Muratore, G. Prestopino, B. Pignataro, G. Lazzara, G. Arrabito and A. Pettignano, Label-free impedimetric analysis of microplastics dispersed in aqueous media polluted by Pb^{2+} ions, *Anal. Methods*, 2024, **16**, 7654–7666.

3 M. Hamzah, M. Fawzi, B. Mfarrej and K. Ali, Science of the Total Environment Emerging trends in wastewater treatment: addressing microorganic pollutants and environmental impacts, *Sci. Total Environ.*, 2024, **913**, 169755.

4 S. Kathi, A. El and D. Mahmoud, Trends in effective removal of emerging contaminants from wastewater: a comprehensive review, *Desalin. Water Treat.*, 2024, **317**, 100258.

5 H. Zhou, C. C. Mayorga-Martinez, S. Pané, L. Zhang and M. Pumera, Magnetically Driven Micro and Nanorobots, *Chem. Rev.*, 2021, **121**, 4999–5041.

6 J. Yi Hou, H. Tao Liu, L. Ting Huang, S. Biao Wu and Z. Lin Zhang, Recent advances in micro/nano-robots for environmental pollutant removal: mechanism, application, and prospect, *Chem. Eng. J.*, 2024, **498**, 155135.

7 F. Yuan, M. S. Hasan and H. Yu, *Design and Modelling of a Micro Swimming Robot, Int. Conf. Adv. Mechatron. Syst. ICAMechS*, 2019, 2019-August, 384–389.

8 B. Nelson, L. Dong and F. Arai, Micro/Nanorobots, in *Springer Handbook of Robotics*, ed. B. Siciliano, O. Khatib, Springer, Berlin, Heidelberg, 2008, pp. 411–450, DOI: 10.1007/978-3-540-30301-5_19.

9 M. Urso, M. Ussia and M. Pumera, Smart micro- and nanorobots for water purification, *Nat. Rev. Bioeng.*, 2023, **1**, 236–251.

10 J. G. S. Moo and M. Pumera, Chemical Energy Powered Nano/Micro/Macromotors and the Environment, *Chem. – Eur. J.*, 2015, **21**, 58–72.

11 G. Chen, F. Zhu, A. S. J. Gan, B. Mohan, K. K. Dey, K. Xu, G. Huang, J. Cui, A. A. Solovev and Y. Mei, Towards the next generation nanorobots, *Next Nanotechnol.*, 2023, **2**, 100019.

12 S. R. Dabbagh, M. R. Sarabi, M. T. Birtek, S. Seyfi, M. Sitti and S. Tasoglu, 3D-printed microrobots from design to translation, *Nat. Commun.*, 2022, **13**, 5875.

13 B. Wang, K. Kostarelos, B. J. Nelson and L. Zhang, Trends in Micro-/Nanorobotics: Materials Development, Actuation, Localization, and System Integration for Biomedical Applications, *Adv. Mater.*, 2021, **33**, 2002047.

14 Y. Wang, J. Chen, G. Su, J. Mei and J. Li, A Review of Single-Cell Microrobots: Classification, Driving Methods and Applications, *Micromachines*, 2023, **14**, 1710.

15 J. Li and M. Pumera, 3D printing of functional microrobots, *Chem. Soc. Rev.*, 2021, **50**, 2794–2838.

16 J. Li, B. E. F. De Ávila, W. Gao, L. Zhang and J. Wang, Micro/nanorobots for Biomedicine: delivery, surgery, sensing, and detoxification, *Sci. Rob.*, 2017, **2**, 1–9.

17 J. Li, I. Rozen and J. Wang, Rocket Science at the Nanoscale, *ACS Nano*, 2016, **10**, 5619–5634.

18 S. Palagi, A. G. Mark, S. Y. Reigh, K. Melde, T. Qiu, H. Zeng, C. Parmeggiani, D. Martella, A. Sanchez-Castillo, N. Kapernaum, F. Giesselmann, D. S. Wiersma, E. Lauga and P. Fischer, Structured light enables biomimetic swimming and versatile locomotion of photoresponsive soft microrobots, *Nat. Mater.*, 2016, **15**, 647–653.

19 S. Palagi and P. Fischer, Bioinspired microrobots, *Nat. Rev. Mater.*, 2018, **3**, 113–124.

20 U. Bozuyuk, O. Yasa, I. C. Yasa, H. Ceylan, S. Kizilel and M. Sitti, Light-Triggered Drug Release from 3D-Printed Magnetic Chitosan Microswimmers, *ACS Nano*, 2018, **12**, 9617–9625.

21 K. Yang, S. Won, J. E. Park, J. Jeon and J. J. Wie, Magnetic swarm intelligence of mass-produced, programmable microrobot assemblies for versatile task execution, *Device*, 2024, **3**(4), 100626.

22 N. Senthilnathan, C. M. Oral and M. Pumera, Magneto-Fluorescent Microrobots with Selective Detection Intelligence for High-Energy Explosives and Antibiotics in Aqueous Environments, *ACS Appl. Mater. Interfaces*, 2025, **17**, 21691–21704.

23 R. Maria-Hormigos, C. C. Mayorga-Martinez, J. Kim and M. Pumera, High-throughput Photoactive Magnetic Microrobots for Food Quality Control, *Small Methods*, 2025, **9**, 2401952.

24 D.-D. Zhou, Q.-X. Hou, W. Liu and Q. Feng, Selectively removing lignin from pre-hydrolysis liquor by combined CaO/PAC method, *Chem. Ind. For. Prod.*, 2016, **36**, 75–80.

25 Z. Geng, T. Deng, B. Gu, X. Qian, R. Li, L. Duan, J. Li, W. Han, L. Qu and K. Wei, Visible-light-sensitive microrobots using H_2O as fuel for highly efficient capture and precise detection of nanoplastics, *J. Hazard. Mater.*, 2024, **479**, 135731.

26 M. Ikram, C. Hu, Y. Zhou and Y. Gao, Bimetallic Photo-Activated and Steerable Janus Micromotors as Active Microcleaners for Wastewater, *ACS Appl. Mater. Interfaces*, 2024, **16**, 33439–33450.

27 Y. Yuan, X. Wu, B. Kalleshappa and M. Pumera, Light-Programmable g-C_3N_4 Microrobots with Negative Photogravitaxis for Photocatalytic Antibiotic Degradation, *Research*, 2025, **8**, 0565.

28 V. Magdanz, G. Stoychev, L. Ionov, S. Sanchez and O. G. Schmidt, Stimuli-Responsive Microjets with Reconfigurable Shape, *Angew. Chem., Int. Ed.*, 2014, **53**, 2673–2677.

29 A. Panda, A. S. Reddy, S. Venkateswarlu and M. Yoon, Bio-inspired self-propelled diatom micromotor by catalytic decomposition of H_2O_2 under low fuel concentration, *Nanoscale*, 2018, **10**, 16268–16277.

30 X. Peng, H. Zhu, H. Chen, X. Feng, R. Liu, Z. Huang, Q. Shen, Y. Ma and L. Wang, Eco-friendly porous iron(III) oxide micromotors for efficient wastewater cleaning, *New J. Chem.*, 2019, **43**, 12594–12600.

31 X. Liu, Y. Peng, Z. Yan, D. Cao, S. Duan and W. Wang, Oscillations of the Local pH Reverses Silver Micromotors in H_2O_2, *ChemSystemsChem*, 2024, **202400046**, 1–7.

This journal is © The Royal Society of Chemistry 2025

J. Mater. Chem. C, 2025, **13**, 19576–19600 | **19595**

32 Z. Xiao, M. Voigtmann and J. Simmchen, Biomimetic Chemotactic Motion of Self-Assembling Doublet Microrobots, *Adv. Intell. Syst.*, 2025, 2400839.

33 J. Li, T. Li, T. Xu, M. Kiristi, W. Liu, Z. Wu and J. Wang, Magneto–Acoustic Hybrid Nanomotor, *Nano Lett.*, 2015, **15**, 4814–4821.

34 X. Peng, M. Urso, M. Kolackova, D. Huska and M. Pumera, Biohybrid Magnetically Driven Microrobots for Sustainable Removal of Micro/Nanoplastics from the Aquatic Environment, *Adv. Funct. Mater.*, 2024, **34**, 2307477.

35 Y. Li, D. Li, Y. Zheng, S. Lu, Y. Cai and R. Dong, Biohybrid microrobots with a Spirulina skeleton and MOF skin for efficient organic pollutant adsorption, *Nanoscale*, 2025, **17**, 7035–7044.

36 J. Wang, Y. Xing, M. Ngatio, P. Bies, L. L. Xu, L. Xing, A. Zarea, A. V. Makela, C. H. Contag and J. Li, Engineering Magnetotactic Bacteria as Medical Microrobots, *Adv. Mater.*, 2025, **37**(27), 2416966.

37 S. Cranford, Materiomics: biological protein materials, from nano to macro, *Nanotechnol., Sci. Appl.*, 2010, **3**, 127–148.

38 B. Zhu, A. Salehi, L. Xu, W. Yuan and T. Yu, Multi-Module Micro/Nanorobots for Biomedical and Environmental Remediation Applications, *Adv. Intell. Syst.*, 2025, **7**, DOI: 10.1002/aisy.202400779.

39 K. Villa, Exploring innovative designs and heterojunctions in photocatalytic micromotors, *Chem. Commun.*, 2023, **59**, 8375–8383.

40 C. Chen, S. Ding and J. Wang, Materials consideration for the design, fabrication and operation of microscale robots, *Nat. Rev. Mater.*, 2024, **9**, 159–172.

41 S. Cataldo, B. M. Weckhuysen, A. Pettignano and B. Pignataro, Multi-doped Brookite-Prevalent TiO_2 Photocatalyst with Enhanced Activity in the Visible Light, *Catal. Lett.*, 2018, **148**, 2459–2471.

42 C. Chiappara, G. Arrabito, V. Ferrara, M. Scopelliti, G. Sancataldo, V. Vetri, D. F. Chillura Martino and B. Pignataro, Improved Photocatalytic Activity of Polysiloxane TiO_2 Composites by Thermally Induced Nanoparticle Bulk Clustering and Dye Adsorption, *Langmuir*, 2021, **37**, 10354–10365.

43 V. Ferrara, M. Marchetti, D. Alfieri, L. Targetti, M. Scopelliti, B. Pignataro, F. Pavone, V. Vetri and G. Sancataldo, Blue light activated photodegradation of biomacromolecules by N-doped titanium dioxide in a chitosan hydrogel matrix, *J. Photochem. Photobiol., A*, 2023, **437**, 114451.

44 J. Zhang, J. Song, F. Mou, J. Guan and A. Sen, Titania-Based Micro/Nanomotors: Design Principles, Biomimetic Collective Behavior, and Applications, *Trends Chem.*, 2021, **3**, 387–401.

45 X. Wang, V. Sridhar, S. Guo, N. Talebi, A. Miguel-lópez, K. Hahn, P. A. Van Aken and S. Sánchez, Fuel-Free Nanocap-Like Motors Actuated Under Visible Light, *Adv. Funct. Mater.*, 2018, **1705862**, 1–7.

46 J. Lin, Y. Tao, J. Liu, C. Zheng, X. Song, P. Dai, Q. Wang, W. Li and W. Chen, TiO_2@carbon microsphere core–shell micromotors for photocatalytic water remediation, *Opt. Mater.*, 2022, **124**, 111989.

47 É. O'Neel-Judy, D. Nicholls, J. Castañeda and J. G. Gibbs, Light-Activated, Multi-Semiconductor Hybrid Microswimmers, *Small*, 2018, **14**, 1–6.

48 M. Urso, M. Ussia, X. Peng, C. M. Oral and M. Pumera, Reconfigurable self-assembly of photocatalytic magnetic microrobots for water purification, *Nat. Commun.*, 2023, **14**, 1–13.

49 V. Sridhar, B. W. Park, S. Guo, P. A. Van Aken and M. Sitti, Multiwavelength-Steerable Visible-Light-Driven Magnetic CoO–TiO_2 Microswimmers, *ACS Appl. Mater. Interfaces*, 2020, **12**, 24149–24155.

50 R. Ferrer Campos, A. C. Bakenecker, Y. Chen, M. C. Spadaro, J. Fraire, J. Arbiol, S. Sánchez and K. Villa, Boosting the Efficiency of Photoactive Rod-Shaped Nanomotors via Magnetic Field-Induced Charge Separation, *ACS Appl. Mater. Interfaces*, 2024, **16**, 30077–30087.

51 P. Chattopadhyay, S. Heckel, F. Irigon Pereira and J. Simmchen, A Path toward Inherently Asymmetric Micromotors, *Adv. Intell. Syst.*, 2023, **5**, 1–6.

52 J. R. Stetter and J. Li, Amperometric Gas Sensors A Review, *Chem. Rev.*, 2008, **108**, 352–366.

53 S. Anselmo, G. De Luca, V. Ferrara, B. Pignataro, G. Sancataldo and V. Vetri, Insight into mechanisms of creatinine optical sensing using fluorescein–gold complex, *Methods Appl. Fluoresc.*, 2022, **10**, 045003.

54 S. He, Y. Gui, Y. Wang, L. Cao, G. He and C. Tang, CuO/TiO_2/MXene-Based Sensor and SMS-TENG Array Integrated Inspection Robots for Self-Powered Ethanol Detection and Alarm at Room Temperature, *ACS Sens.*, 2024, **9**, 1188–1198.

55 A. Jancik-Prochazkova, H. Kmentova, X. Ju, S. Kment, R. Zboril and M. Pumera, Precision Engineering of Nanorobots: Toward Single Atom Decoration and Defect Control for Enhanced Microplastic Capture, *Adv. Funct. Mater.*, 2024, **2402567**, 1–11.

56 M. Wittmann, A. Ali, T. Gemming, F. Stavale and J. Simmchen, Semiconductor-Based Microswimmers: Attention to Detail Matters, *J. Phys. Chem. Lett.*, 2021, **12**, 9651–9656.

57 M. Urso, L. Bruno, S. Dattilo, S. C. Carroccio and S. Mirabella, Band Engineering versus Catalysis: Enhancing the Self-Propulsion of Light-Powered MXene-Derived Metal–TiO_2 Micromotors To Degrade Polymer Chains, *ACS Appl. Mater. Interfaces*, 2024, **16**, 1293–1307.

58 G. Arrabito, G. Prestopino, P. G. Medaglia, V. Ferrara, G. Sancataldo, G. Cavallaro, F. Di Franco, M. Scopelliti and B. Pignataro, Freestanding cellulose acetate/ZnO flowers composites for solar photocatalysis and controlled zinc ions release, *Colloids Surf., A*, 2024, **698**, 134526.

59 A. M. Pourrahimi, K. Villa, Y. Ying, Z. Sofer and M. Pumera, ZnO/ZnO_2/Pt Janus Micromotors Propulsion Mode Changes with Size and Interface Structure: Enhanced Nitroaromatic Explosives Degradation under Visible Light, *ACS Appl. Mater. Interfaces*, 2018, **10**, 42688–42697.

60 C. M. Oral, M. Ussia and M. Pumera, Hybrid Enzymatic/Photocatalytic Degradation of Antibiotics via Morphologically Programmable Light-Driven ZnO Microrobots, *Small*, 2022, **18**, 1–8.

19596 | *J. Mater. Chem. C*, 2025, **13**, 19576–19600

This journal is © The Royal Society of Chemistry 2025

61 P. Moradipour, A. Ali Khodadadi, Y. Mortazavi and A. Javadi, Janus ZnO microrod-spherical carbon artificial bacteriabot micromotors driven by photocatalytic water splitting, corrosion, and thermal buoyancy, *Chem. Eng. Sci.*, 2024, **294**, 120107.

62 M. Ussia, M. Urso, K. Dolezelikova, H. Michalkova, V. Adam and M. Pumera, Active Light-Powered Antibiofilm ZnO Micromotors with Chemically Programmable Properties, *Adv. Funct. Mater.*, 2021, **31**, 1–10.

63 F. Mou, Q. Xie, J. Liu, S. Che, L. Bahmane, M. You and J. Guan, ZnO-based micromotors fueled by CO_2: the first example of self-reorientation-induced biomimetic chemotaxis, *Natl. Sci. Rev.*, 2021, **8**(11), nwab066.

64 P. K. Mishra, H. Mishra, A. Ekielski, S. Talegaonkar and B. Vaidya, Zinc oxide nanoparticles: a promising nanomaterial for biomedical applications, *Drug Discovery Today*, 2017, **22**, 1825–1834.

65 G. Arrabito, Y. Aleeva, V. Ferrara, G. Prestopino, C. Chiappara and B. Pignataro, On the interaction between 1d materials and living cells, *J. Funct. Biomater.*, 2020, **11**(2), 40.

66 D. Gong, N. Celi, L. Xu, D. Zhang and J. Cai, CuS nanodots-loaded biohybrid magnetic helical microrobots with enhanced photothermal performance, *Mater. Today Chem.*, 2022, **23**, 100694.

67 H. Tan, B. Chen, M. Liu, J. Jiang, J. Ou, L. Liu, F. Wang, Y. Ye, J. Gao, J. Sun, F. Peng and Y. Tu, Adaptive Cu_2O micromotors with pH-responsive phototaxis reversal, *Chem. Eng. J.*, 2022, **448**, 137689.

68 S. Sánchez, L. Soler and J. Katuri, Chemically Powered Micro- and Nanomotors, *Angew. Chem., Int. Ed.*, 2015, **54**, 1414–1444.

69 X. Chen, X. Ding, Y. Liu, J. Li, W. Liu, X. Lu and Z. Gu, Highly efficient visible-light-driven Cu_2O@CdSe micromotors adsorbent, *Appl. Mater. Today*, 2021, **25**, 101200.

70 J. Fu, J. Jiao, W. Ban, Y. Kong, Z. Gu, H. Song, X. Huang, Y. Yang and C. Yu, Large scale synthesis of self-assembled shuttlecock-shaped silica nanoparticles with minimized drag as advanced catalytic nanomotors, *Chem. Eng. J.*, 2021, **417**, 127971.

71 H. Shen, S. Cai, Z. Wang, Z. Ge and W. Yang, Magnetically driven microrobots: recent progress and future development, *Mater. Des.*, 2023, **227**, 111735.

72 W. Wang, Y. He, H. Liu, Q. Guo, Z. Ge and W. Yang, Bubble-based microrobot: recent progress and future perspective, *Sens. Actuators, A*, 2023, **360**, 114567.

73 L. Chen, X. Sun, H. Wang and Z. Zhang, Preparation of dual-drive hybrid micromotors by swelling and selective surface modification of polymeric colloids, *Colloids Interface Sci. Commun.*, 2020, **38**, 100300.

74 J. Li, X. He, H. Jiang, Y. Xing, B. Fu and C. Hu, Enhanced and Robust Directional Propulsion of Light-Activated Janus Micromotors by Magnetic Spinning and the Magnus Effect, *ACS Appl. Mater. Interfaces*, 2022, **14**, 36027–36037.

75 Q. Fu, S. Guo, S. Zhang, H. Hirata and H. Ishihara, Characteristic evaluation of a shrouded propeller mechanism

for a magnetic actuated microrobot, *Micromachines*, 2015, **6**, 1272–1288.

76 S. Alipoori, H. Rouhi, E. Linn, H. Stumpfl, H. Mokarizadeh, M. R. Esfahani, A. Koh, S. T. Weinman and E. K. Wujcik, Polymer-Based Devices and Remediation Strategies for Emerging Contaminants in Water, *ACS Appl. Polym. Mater.*, 2021, **3**, 549–577.

77 N. Lin, J. Huang and A. Dufresne, Preparation, properties and applications of polysaccharide nanocrystals in advanced functional nanomaterials: a review, *Nanoscale*, 2012, **4**, 3274–3294.

78 A. De Nino, M. A. Tallarida, V. Algieri, F. Olivito, P. Costanzo, G. De Filpo and L. Maiuolo, Sulfonated cellulose-based magnetic composite as useful media for water remediation from amine pollutants, *Appl. Sci.*, 2020, **10**(22), 1–15.

79 V. Algieri, A. Tursi, P. Costanzo, L. Maiuolo, A. De Nino, A. Nucera, M. Castriota, O. De Luca, M. Papagno, T. Caruso, S. Ciurciù, G. A. Corrente and A. Beneduci, Thiol-functionalized cellulose for mercury polluted water remediation: synthesis and study of the adsorption properties, *Chemosphere*, 2024, **355**, 141891.

80 Y. Cui, J. Lin, Y. Wu, M. Chen, X. Yang and C. Chang, Nanocellulose-based soft actuators and their applications, *J. Polym. Sci.*, 2024, **62**, 280–296.

81 Y. Liu, S. Shang, S. Mo, P. Wang, B. Yin and J. Wei, Soft actuators built from cellulose paper: a review on actuation, material, fabrication, and applications, *J. Sci.: Adv. Mater. Devices*, 2021, **6**, 321–337.

82 N. Gariya and P. Kumar, A review on soft materials utilized for the manufacturing of soft robots, *Mater. Today Proc.*, 2021, **46**, 11177–11181.

83 W. Chen, B. Sun, P. Biehl and K. Zhang, Cellulose-Based Soft Actuators, *Macromol. Mater. Eng.*, 2022, **307**, 2200072.

84 Y. Li, C. Fu, L. Huang, L. Chen, Y. Ni and Q. Zheng, Cellulose-based multi-responsive soft robots for programmable smart devices, *Chem. Eng. J.*, 2024, **498**, 155099.

85 T. Wu, J. Li, J. Li, S. Ye, J. Wei and J. Guo, A bio-inspired cellulose nanocrystal-based nanocomposite photonic film with hyper-reflection and humidity-responsive actuator properties, *J. Mater. Chem. C*, 2016, **4**, 9687–9696.

86 S.-S. Kim, J.-H. Jeon, C.-D. Kee and I.-K. Oh, Electro-active hybrid actuators based on freeze-dried bacterial cellulose and PEDOT:PSS, *Smart Mater. Struct.*, 2013, **22**, 85026.

87 M. Amjadi and M. Sitti, High-Performance Multiresponsive Paper Actuators, *ACS Nano*, 2016, **10**, 10202–10210.

88 R. Nasseri, N. Bouzari, J. Huang, H. Golzar, S. Jankhani, X. (Shirley) Tang, T. H. Mekonnen, A. Aghakhani and H. Shahsavan, Programmable nanocomposites of cellulose nanocrystals and zwitterionic hydrogels for soft robotics, *Nat. Commun.*, 2023, **14**, 6108.

89 M. Naguib, M. Kurtoglu, V. Presser, J. Lu, J. Niu, M. Heon, L. Hultman, Y. Gogotsi and M. W. Barsoum, Two-Dimensional Nanocrystals Produced by Exfoliation of Ti_3AlC_2, *Adv. Mater.*, 2011, **23**, 4248–4253.

90 J. Qin, J. Li, G. Yang, K. Chu, L. Zhang, F. Xu, Y. Chen, Y. Zhang, W. Fan, J. Hofkens, B. Li, Y. Zhu, H. Wu, S. C. Tan,

This journal is © The Royal Society of Chemistry 2025

J. Mater. Chem. C, 2025, **13**, 19576–19600 | **19597**

F. Lai and T. Liu, A Bio-Inspired Magnetic Soft Robotic Fish for Efficient Solar-Energy Driven Water Purification, *Small Methods*, 2025, **9**, 2400880.

91 A. Nwabike Amitaye, E. E. Elemike, H. B. Akpeji, E. Amitaye, I. Hossain, J. I. Mbonu and A. E. Aziza, Chitosan: a sustainable biobased material for diverse applications, *J. Environ. Chem. Eng.*, 2024, **12**, 113208.

92 J. Zhang, Y. Guo, Y. Yang, N. Fu, S. Wang and Z. Deng, Self-Cleaning MXene/Bacterial Cellulose Composite Film for Photothermal Actuation and Sterilization, *ACS Appl. Nano Mater.*, 2024, **7**, 27531–27542.

93 Q. Wang, Z. Wang, Y. Tao, P. Liu, Y. Huang, J. Du, J. Hu, J. Lu, Y. Lv and H. Wang, Redox active metallene anchored amino-functionalized cellulose composite for electrochemical capture and conversion of chromium, *Int. J. Biol. Macromol.*, 2024, **282**, 137310.

94 V. Sridhar, F. Podjaski, J. Kröger, A. Jiménez-Solano, B. W. Park, B. V. Lotsch and M. Sitti, Carbon nitride-based light-driven microswimmers with intrinsic photocharging ability, *Proc. Natl. Acad. Sci. U. S. A.*, 2020, **117**, 24748–24756.

95 R. Maria-Hormigos, C. C. Mayorga-Martinez and M. Pumera, Soft Magnetic Microrobots for Photoactive Pollutant Removal, *Small Methods*, 2023, **7**, 1–9.

96 B. Okmen Altas, C. Goktas, G. Topcu and N. Aydogan, Multi-Stimuli-Responsive Tadpole-like Polymer/Lipid Janus Microrobots for Advanced Smart Material Applications, *ACS Appl. Mater. Interfaces*, 2024, **16**, 15533–15547.

97 M. Ussia, M. Urso, C. M. Oral, X. Peng and M. Pumera, Magnetic Microrobot Swarms with Polymeric Hands Catching Bacteria and Microplastics in Water, *ACS Nano*, 2024, **18**, 13171–13183.

98 R. Dong, Y. Hu, Y. Wu, W. Gao, B. Ren, Q. Wang and Y. Cai, Visible-light-driven BiOI-based janus micromotor in pure water, *J. Am. Chem. Soc.*, 2017, **139**, 1722–1725.

99 K. Khairudin, N. F. Abu Bakar and M. S. Osman, Magnetically recyclable flake-like BiOI–Fe$_3$O$_4$ microswimmers for fast and efficient degradation of microplastics, *J. Environ. Chem. Eng.*, 2022, **10**, 108275.

100 K. Villa, F. Novotný, J. Zelenka, M. P. Browne, T. Ruml and M. Pumera, Visible-Light-Driven Single-Component BiVO$_4$ Micromotors with the Autonomous Ability for Capturing Microorganisms, *ACS Nano*, 2019, **13**, 8135–8145.

101 P. Mayorga-Burrezo, C. C. Mayorga-Martinez and M. Pumera, Light-Driven Micromotors to Dissociate Protein Aggregates That Cause Neurodegenerative Diseases, *Adv. Funct. Mater.*, 2022, **32**, 1–8.

102 S. Heckel and J. Simmchen, Photocatalytic BiVO$_4$ Microswimmers with Bimodal Swimming Strategies, *Adv. Intell. Syst.*, 2019, **1**(8), 1900093.

103 S. Heckel, J. Grauer, M. Semmler, T. Gemming, H. Löwen, B. Liebchen and J. Simmchen, Active assembly of spheroidal photocatalytic BiVO$_4$ microswimmers, *Langmuir*, 2020, **36**, 12473–12480.

104 Z. Chen, J. Jiang, X. Wang, H. Zhang, B. Song and B. Dong, Visible light-regulated BiVO$_4$-based micromotor with biomimetic 'predator-bait' behavior, *J. Mater. Sci.*, 2022, **57**, 4092–4103.

105 P. Mayorga-Burrezo, C. C. Mayorga-Martinez and M. Pumera, Photocatalysis dramatically influences motion of magnetic microrobots: application to removal of microplastics and dyes, *J. Colloid Interface Sci.*, 2023, **643**, 447–454.

106 K. Villa, L. Děkanovský, J. Plutnar, J. Kosina and M. Pumera, Swarming of Perovskite-Like Bi$_2$WO$_6$ Microrobots Destroy Textile Fibers under Visible Light, *Adv. Funct. Mater.*, 2020, **30**, 1–10.

107 S. Virga, G. Arrabito, V. Ferrara, M. Scopelliti, A. Longo, B. Pignataro and F. Giannici, Bismuth drives the morphology and piezoresistivity of lead-free (TMSO)$_3$Sn$_{3x}$Bi$_{2(1−x)}$I$_9$ halide perovskite thin films, *J. Mater. Chem. C*, 2024, **12**, 12951–12961.

108 H. Wang, J. Xiong, Y. Cai, W. Fu, Y. Zhong, T. Jiang and U. K. Cheang, Stabilization of CsPbBr$_3$ Nanowires Through SU-8 Encapsulation for the Fabrication of Bilayer Microswimmers with Magnetic and Fluorescence Properties, *Small*, 2024, **2400346**, 1–12.

109 M. Chen, Z. Lin, M. Xuan, X. Lin, M. Yang, L. Dai and Q. He, Programmable Dynamic Shapes with a Swarm of Light-Powered Colloidal Motors, *Angew. Chem., Int. Ed.*, 2021, **60**, 16674–16679.

110 V. de la Asunción-Nadal, E. Solano, B. Jurado-Sánchez and A. Escarpa, Photophoretic MoS$_2$–Fe$_2$O$_3$ Piranha Micromotors for Collective Dynamic Microplastics Removal, *ACS Appl. Mater. Interfaces*, 2024, **16**, 47396–47405.

111 M. Urso, M. Ussia, F. Novotný and M. Pumera, Trapping and detecting nanoplastics by MXene-derived oxide microrobots, *Nat. Commun.*, 2022, **13**, 1–14.

112 A. Jancik-Prochazkova and M. Pumera, Light-powered swarming phoretic antimony chalcogenide-based microrobots with "on-the-fly" photodegradation abilities, *Nanoscale*, 2023, **15**, 5726–5734.

113 A. Jancik-Prochazkova, V. Jašek, S. Figalla and M. Pumera, Photocatalytic Microplastics "On-The-fly" Degradation via Motile Quantum Materials-Based Microrobots, *Adv. Opt. Mater.*, 2023, **11**, 1–9.

114 V. de la Asunción-Nadal, D. Rojas, B. Jurado-Sánchez and A. Escarpa, Transition metal dichalcogenide micromotors with programmable photophoretic swarming motion, *J. Mater. Chem. A*, 2023, **11**, 1239–1245.

115 H. Chen, Z. Zheng, H. Yu, D. Qiao, D. Feng, Z. Song and J. Zhang, Preparation and Tribological Properties of MXene-Based Composite Films, *Ind. Eng. Chem. Res.*, 2021, **60**, 11128–11140.

116 P. Malgaretti, M. N. Popescu and S. Dietrich, Self-diffusiophoresis induced by fluid interfaces, *Soft Matter*, 2018, **14**, 1375–1388.

117 X. Wang, M. In, C. Blanc, M. Nobili and A. Stocco, Enhanced active motion of Janus colloids at the water surface, *Soft Matter*, 2015, **11**, 7376–7384.

118 V. Ferrara, G. Zito, G. Arrabito, S. Cataldo, M. Scopelliti, C. Giordano, V. Vetri and B. Pignataro, Aqueous processed biopolymer interfaces for single-cell microarrays, *ACS Biomater. Sci. Eng.*, 2020, **6**, 3174–3186.

119 G. Arrabito, V. Errico, A. De Ninno, F. Cavaleri, V. Ferrara, B. Pignataro and F. Caselli, Oil-in-water fL droplets by

19598 | *J. Mater. Chem. C*, 2025, **13**, 19576–19600

This journal is © The Royal Society of Chemistry 2025

interfacial spontaneous fragmentation and their electrical characterization, *Langmuir*, 2019, **35**, 4936–4945.

120 G. Arrabito, F. Cavaleri, A. Porchetta, F. Ricci, V. Vetri, M. Leone and B. Pignataro, Printing Life-Inspired Subcellular Scale Compartments with Autonomous Molecularly Crowded Confinement, *Adv. Biosyst.*, 2019, **3**, 1–11.

121 M. B. Akolpoglu, Y. Alapan, N. O. Dogan, S. F. Baltaci, O. Yasa, G. A. Tural and M. Sitti, Magnetically steerable bacterial microrobots moving in 3D biological matrices for stimuli-responsive cargo delivery, *Sci. Adv.*, 2022, **8**, 1–14.

122 J. Liu, Z. Yang, Z. Yan, S. Duan, X. Chen, D. Cui, D. Cao, T. Kuang, X. Ma and W. Wang, Chemical Micromotors Move Faster at Oil–Water Interfaces, *J. Am. Chem. Soc.*, 2024, **146**, 4221–4233.

123 H. Hao, I. Leven and T. Head-Gordon, Can electric fields drive chemistry for an aqueous microdroplet?, *Nat. Commun.*, 2022, **13**, 1–8.

124 Z. Wei, Y. Li, R. G. Cooks and X. Yan, Accelerated reaction kinetics in microdroplets: overview and recent developments, *Annu. Rev. Phys. Chem.*, 2020, **71**, 31–51.

125 A. Arslanova, I. Matthé, O. Deschaume, C. Bartic, W. Monnens, E. K. Reichel, N. Reddy, J. Fransaer and C. Clasen, Sideways propelled bimetallic rods at the water/oil interface, *Soft Matter*, 2023, **19**, 6896–6902.

126 R. K. Liu, Y. Guo, J. Jia, Q. Sun, H. Zhao and J. X. Wang, Asymmetric Assembly in Microdroplets: Efficient Construction of MOF Micromotors for Anti-Gravity Diffusion, *Small*, 2024, **2402819**, 1–8.

127 S. K. Choudhary, A. Baskaran and P. Sharma, Reentrant Efficiency of Phototaxis in Chlamydomonas reinhardtii Cells, *Biophys. J.*, 2019, **117**, 1508–1513.

128 M. B. Akolpoglu, N. O. Dogan, U. Bozuyuk, H. Ceylan, S. Kizilel and M. Sitti, High-Yield Production of Biohybrid Microalgae for On-Demand Cargo Delivery, *Adv. Sci.*, 2020, **7**, 1–10.

129 D. Kim, A. Liu, E. Diller and M. Sitti, Chemotactic steering of bacteria propelled microbeads, *Biomed. Microdevices*, 2012, **14**, 1009–1017.

130 J. Zhuang and M. Sitti, Chemotaxis of bio-hybrid multiple bacteria-driven microswimmers, *Sci. Rep.*, 2016, **6**, 1–10.

131 Y. Alapan, O. Yasa, O. Schauer, J. Giltinan, A. F. Tabak, V. Sourjik and M. Sitti, Soft erythrocyte-based bacterial microswimmers for cargo delivery, *Sci. Rob.*, 2018, **3**, eaar4423.

132 B. Behkam and M. Sitti, Bacterial flagella-based propulsion and on/off motion control of microscale objects, *Appl. Phys. Lett.*, 2007, **90**, 23902.

133 V. Du Nguyen, J. W. Han, Y. J. Choi, S. Cho, S. Zheng, S. Y. Ko, J. O. Park and S. Park, Active tumor-therapeutic liposomal bacteriobot combining a drug (paclitaxel)-encapsulated liposome with targeting bacteria (Salmonella Typhimurium), *Sens. Actuators, B*, 2016, **224**, 217–224.

134 N. S. Forbes, Engineering the perfect (bacterial) cancer therapy, *Nat. Rev. Cancer*, 2010, **10**, 785–794.

135 M. I. S. Naduthodi, N. J. Claassens, S. D'Adamo, J. van der Oost and M. J. Barbosa, Synthetic Biology Approaches To Enhance Microalgal Productivity, *Trends Biotechnol.*, 2021, **39**, 1019–1036.

136 R. W. Carlsen, M. R. Edwards, J. Zhuang, C. Pacoret and M. Sitti, Magnetic steering control of multi-cellular bio-hybrid microswimmers, *Lab Chip*, 2014, **14**, 3850–3859.

137 D. B. Weibel, P. Garstecki, D. Ryan, W. R. DiLuzio, M. Mayer, J. E. Seto and G. M. Whitesides, Microoxen: microorganisms to move microscale loads, *Proc. Natl. Acad. Sci. U. S. A.*, 2005, **102**, 11963–11967.

138 R. W. Carlsen and M. Sitti, Bio-Hybrid Cell-Based Actuators for Microsystems, *Small*, 2014, **10**, 3831–3851.

139 S. Martel, C. C. Tremblay, S. Ngakeng and G. Langlois, Controlled manipulation and actuation of micro-objects with magnetotactic bacteria, *Appl. Phys. Lett.*, 2006, **89**, 233904.

140 A. Krichevsky, M. J. Smith, L. J. Whitman, M. B. Johnson, T. W. Clinton, L. L. Perry, B. M. Applegate, K. O'Connor and L. N. Csonka, Trapping motile magnetotactic bacteria with a magnetic recording head, *J. Appl. Phys.*, 2007, **101**, 14701.

141 H. Wang, Y. Jing, J. Yu, B. Ma, M. Sui, Y. Zhu, L. Dai, S. Yu, M. Li and L. Wang, Micro/nanorobots for remediation of water resources and aquatic life, *Front. Bioeng. Biotechnol.*, 2023, **11**, 1–21.

142 J. Li, L. Dekanovsky, B. Khezri, B. Wu, H. Zhou and Z. Sofer, Biohybrid Micro- and Nanorobots for Intelligent Drug Delivery, *Cyborg Bionic Syst.*, 2022, **2022**, 9824057.

143 P. Gotovtsev, Microbial Cells as a Microrobots: From Drug Delivery to Advanced Biosensors, *Biomimetics*, 2023, **8**, 1–16.

144 L. P. Jahromi, M.-A. Shahbazi, A. Maleki, A. Azadi and H. A. Santos, Chemically Engineered Immune Cell-Derived Microrobots and Biomimetic Nanoparticles: Emerging Biodiagnostic and Therapeutic Tools, *Adv. Sci.*, 2021, **8**, 2002499.

145 E. N. Santos, Á. F. Fazekas, L. Fekete, T. Miklós, T. Gyulavári, S. A. Gokulakrishnan, G. Arthanareeswaran, C. Hodúr, Z. László and G. Veréb, Enhancing membrane performance for oily wastewater treatment: comparison of PVDF composite membranes prepared by coating, blending, and grafting methods using TiO_2, $BiVO_4$, CNT, and PVP, *Environ. Sci. Pollut. Res. Int.*, 2024, **31**, 64578–64595.

146 B. Jurado-Sánchez and J. Wang, Micromotors for environmental applications: a review, *Environ. Sci.: Nano*, 2018, **5**, 1530–1544.

147 W. Gao and J. Wang, The Environmental Impact of Micro/Nanomachines: A Review, *ACS Nano*, 2014, **8**(4), 3170–3180.

148 C. Cuntín-Abal, B. Jurado-Sánchez and A. Escarpa, Micromotors for antimicrobial resistance bacteria inactivation in water systems: opportunities and challenges, *Environ. Sci.: Nano*, 2025, **12**, 967–978.

149 V. Magdanz, V. M. Fomin, S. Sanchez, O. G. Schmidt, I. Nanosciences, I. F. W. Dresden, I. Systems and M. Systems, Self-Propelled Micromotors for Cleaning Polluted Water, *ACS Nano*, 2013, **7**(11), 9611–9620.

150 X. Arqué, X. Andrés, R. Mestre, B. Ciraulo, J. O. Arroyo, R. Quidant, T. Patiño and S. Sánchez, Ionic Species Affect the Self-Propulsion of Urease-Powered Micromotors, *Research*, 2020, 2424972.

151 M. De Corato, T. Patiño, S. Sánchez and I. Pagonabarraga, Self-Propulsion of Active Colloids via Ion Release: Theory and Experiments, *Phys. Rev. Lett.*, 2020, 108001.

152 S. Barreca, I. P. Oliveri, F. Lo Presti, V. Oliveri, S. Giannakis, N. Tuccitto, V. Spampinato and A. Auditore, An innovative "Up-and-Down" adsorption processes for pyrene removal from acid wastewater as new approach in water remediation, *Sep. Purif. Technol.*, 2024, **348**, 127516.

153 F. Soto, E. Karshalev, F. Zhang, B. Esteban Fernandez de Avila, A. Nourhani and J. Wang, Smart Materials for Microrobots, *Chem. Rev.*, 2022, **122**, 5365–5403.

154 Z. H. Shah, B. Wu and S. Das, Multistimuli-responsive microbots: a comprehensive review, *Front. Robot. AI*, 2022, **9**, 1–17.

155 A. Jancik-Prochazkova and K. Ariga, Nano-/Microrobots for Environmental Remediation in the Eyes of Nanoarchitectonics: Toward Engineering on a Single-Atomic Scale, *Research*, 2025, **8**, 624.

156 Y. Choi, C. Park, A. C. Lee, J. Bae, H. Kim, H. Choi, S. Woo Song, Y. Jeong, J. Choi, H. Lee, S. Kwon and W. Park, Photopatterned microswimmers with programmable motion without external stimuli, *Nat. Commun.*, 2021, **12**, 4724.

157 F. M. den Hoed, M. Carlotti, S. Palagi, P. Raffa and V. Mattoli, Evolution of the Microrobots: Stimuli-Responsive Materials and Additive Manufacturing Technologies Turn Small Structures into Microscale Robots, *Micromachines*, 2024, **15**(2), 275.

158 C. Chen, E. Karshalev, J. Guan and J. Wang, Magnesium-Based Micromotors: Water-Powered Propulsion, Multifunctionality, and Biomedical and Environmental Applications, *Small*, 2018, **14**, 1704252.

159 T. Xu, W. Gao, L.-P. Xu, X. Zhang and S. Wang, Fuel-Free Synthetic Micro-/Nanomachines, *Adv. Mater.*, 2017, **29**, 1603250.

160 H. Sun, L. Wang, F. Guo, Y. Shi, L. Li, Z. Xu, X. Yan and W. Shi, Fe-doped g-C_3N_4 derived from biowaste material with Fe–N bonds for enhanced synergistic effect between photocatalysis and Fenton degradation activity in a broad pH range, *J. Alloys Compd.*, 2022, **900**, 163410.

161 H. Jiang, X. He, M. Yang and C. Hu, Visible Light-Driven Micromotors in Fuel-Free Environment with Promoted Ion Tolerance, *Nanomaterials*, 2023, **13**, 12.

162 S. Sourani and M. Bayareh, From theory to application: exploring the motion dynamics of microrobots, *Microchem. J.*, 2025, **209**, 112846.

163 A. Testa, M. Dindo, A. A. Rebane, B. Nasouri, R. W. Style, R. Golestanian, E. R. Dufresne and P. Laurino, Sustained enzymatic activity and flow in crowded protein droplets, *Nat. Commun.*, 2021, **12**, 1–8.

164 B. Dai, J. Wang, Z. Xiong, X. Zhan, W. Dai, C.-C. Li, S.-P. Feng and J. Tang, Programmable artificial phototactic microswimmer, *Nat. Nanotechnol.*, 2016, **11**, 1087–1092.

165 T. Hou, S. Yu, M. Zhou, M. Wu, J. Liu, X. Zheng, J. Li, J. Wang and X. Wang, Effective removal of inorganic and organic heavy metal pollutants with poly(amino acid)-based micromotors, *Nanoscale*, 2020, **12**, 5227–5232.

166 D. Vilela, J. Parmar, Y. Zeng, Y. Zhao and S. Sánchez, Graphene-Based Microbots for Toxic Heavy Metal Removal and Recovery from Water, *Nano Lett.*, 2016, **16**, 2860–2866.

167 D. Vilela, M. Guix, J. Parmar, À. Blanco-Blanes and S. Sánchez, Micromotor-in-Sponge Platform for Multicycle Large-Volume Degradation of Organic Pollutants, *Small*, 2022, **18**, 1–8.

168 J. Yu, D. Jin, K. F. Chan, Q. Wang, K. Yuan and L. Zhang, Active generation and magnetic actuation of microrobotic swarms in bio-fluids, *Nat. Commun.*, 2019, **10**, 1–12.

169 G. Gardi, S. Ceron, W. Wang, K. Petersen and M. Sitti, Microrobot collectives with reconfigurable morphologies, behaviors, and functions, *Nat. Commun.*, 2022, **13**, 1–14.

170 S. A. Abbasi, A. Ahmed, S. Noh, N. L. Gharamaleki, S. Kim, A. M. M. B. Chowdhury, J. Kim, S. Pané, B. J. Nelson and H. Choi, Autonomous 3D positional control of a magnetic microrobot using reinforcement learning, *Nat. Mach. Intell.*, 2024, **6**, 92–105.

171 V.-L. Heuthe, E. Panizon, H. Gu and C. Bechinger, Counterfactual rewards promote collective transport using individually controlled swarm microrobots, *Sci. Rob.*, 2025, **9**, eado5888.

19600 | *J. Mater. Chem. C*, 2025, **13**, 19576–19600

This journal is © The Royal Society of Chemistry 2025